

638

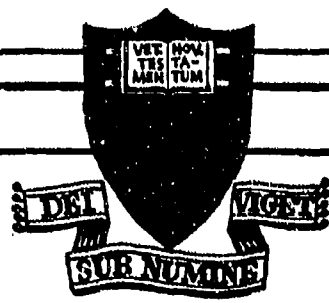
Copy 4

NOV 19 1983

①

AD A 952020

AN EXPERIMENTAL INVESTIGATION
 OF LAMINAR HYPERSONIC CAVITY FLOWS
 Part I: Pressure measurements
 K. M. Nicoll
 Princeton University
 Report 638 December 1962



Suppl
AD-407052

PRINCETON UNIVERSITY
 THE JAMES FORRESTAL
 RESEARCH CENTER
 LIBRARY

DTIC
 ELECTE
 SEP 8 1983
 S D B

PRINCETON UNIVERSITY
 DEPARTMENT OF AERONAUTICAL ENGINEERING

DTIC FILE COPY

DISTRIBUTION STATEMENT A
 Approved for public release
 Distribution Unlimited

88 09 02 136

ARL-63-73

AN EXPERIMENTAL INVESTIGATION
OF LAMINAR HYPERSONIC CAVITY FLOWS
Part I: Pressure measurements

K. M. Nicoll
Princeton University
Report 638 December 1962

DTIC
ELECTE
SEP 8 1983
S B D

Contract AF 33(616)-7629
Project No. 7064
Task No. 70169

Aeronautical Research Laboratory
Office of Aerospace Research
United States Air Force
Wright-Patterson Air Force Base, Ohio

DISTRIBUTION STATEMENT A

Approved for public release;
Distribution Unlimited

ABSTRACT

An experimental investigation has been made of the pressure distributions on a set of cone-models incorporating annular cavities. This study is the first part of a program which includes measurements of recovery factor and heat-transfer distributions. The cone-surface Mach number was 6.5, and all cavity flows were "open".

The results indicate that a regime of laminar, open cavity flow exists at hypersonic Mach number which is characterized by the property that the cavity floor pressure is virtually constant. Recompression is confined to the last 10% of the cavity near the reattachment point.

TABLE OF CONTENTS

I. INTRODUCTION	1
II. EXPERIMENTAL EQUIPMENT AND TECHNIQUES. .	4
III. RESULTS OF EXPERIMENTS	6
IV. COMPARISONS WITH OTHER INVESTIGATIONS. .	13
V. CONCLUDING REMARKS	15
REFERENCES	17

NOTATION

D	Maximum depth of cavity
L	Length of cavity
L_1	Length of model surface before separation shoulder, measured along slant side of cone
M	Mach number
\bar{M}	Mach number on dividing streamline
p	Pressure
Re	Reynolds number based on fluid properties at the edge of the boundary layer on the basic cone
u	Velocity in x direction
u_*	Ratio of u to velocity at edge of shear layer
x	Distance measured from nose along slant side of basic cone
\bar{x}	Distance parameter defined in text
δ	Boundary layer thickness
γ	Ratio of specific heats
ρ	Mass density
μ	Viscosity coefficient

Subscripts:

c, cone	Values on basic cone
Cr	"Critical" value
e	Conditions at edge of boundary or shear layer
o	Isentropic stagnation conditions
R	Reattachment shoulder
R_1	Cavity floor at beginning of reattachment corner radius
R_2	Position of last pressure orifice in cavity before reattachment shoulder
S	Separation shoulder
S_1	Cavity floor at end of separation corner radius
∞	Free-stream conditions

V

Separated flows at supersonic and hypersonic Mach numbers have been the subject of many experimental and theoretical investigations during the past decade. The increasing attention paid to these flows is due partly to their very widespread occurrence, and partly to the extreme modifications of the pressure and heat-transfer distributions which are produced in a flow configuration by a separated region.

At the Gas Dynamics Laboratory of Princeton University, a general program of research into various types of separated flow has been in progress for some time. The present work is an interim report on one aspect of this program -- the study of laminar, hypersonic cavity flows. Besides being a logical part of the framework of the main research program, this investigation was motivated in particular by the work of Chapman and his co-workers at the Ames Research Center. In Ref. 1, it was shown that the separated laminar layer is surprisingly stable at higher Mach numbers, and in hypersonic flow the free laminar layer can be almost as stable as an attached laminar boundary layer. As a result, the separated laminar layer, which at lower Mach numbers had been of little more than academic interest because of its rare occurrence, now appeared to be of considerable practical importance in hypersonic flow. In 1956, Chapman published a theoretical investigation (Ref. 2), which produced the result that for the laminar separated flow model he chose, the average heat-transfer rate was only 56% of that which would occur with an attached layer. (This value was for a Prandtl number of 0.72.) In Ref. 3, the experimental work of

Manuscript released by the author (February, 1963) for publication as an ARL Technical Documentary Report.

Larson confirmed Chapman's prediction. This result offered the attractive possibility of using regions of separated flow as a means of alleviating the heat transfer rates in critical areas on hypersonic flight vehicles.

In Larson's work, and in several investigations which followed, the Mach number of the experiments was in the supersonic range, and the present author is unaware of any experimental studies of laminar cavity-flows which were carried out in hypersonic flow. The experiments described in the present report were all made in the hypersonic regime, at a free-stream Mach number of about 11.

The configuration chosen was that of an annular cavity on a 20° total-angle cone (Figure 1). A cone was taken as the basic model, rather than a flat plate, for the following reasons:

- (I) The problems involved in obtaining truly two-dimensional flow would be avoided.
- (II) The high entropy gas passing through the normal section of the bow-wave at the nose would be distributed over as large a model surface as possible. The boundary layer would therefore absorb the entropy layer before the cavity station was reached.
- (III) The pressure on the surface of the basic model would be substantially constant with distance from the nose.
- (IV) The boundary layer would be as thin as possible. (The cone boundary layer is thinner than that on a flat-plate by the factor $\sqrt{3}$.)

The basic cavity geometry was chosen to have a conical floor, with rounded corners to avoid imbedded ring vortices. (See last sketch of Figure 1.) In addition, a cavity model in which the cut-out was formed

from a single circular arc was studied. (Second sketch of Figure 1.) This latter model was tested to check the sensitivity of the pressure and heat-transfer distributions to fairly drastic changes in reattachment shoulder geometry. In addition, it was hoped that the single-arc cavity geometry might approximate the geometry of a "separation bubble", such as that produced in the interaction between a strong shockwave and a laminar boundary-layer. In particular, the streamline reversal would occur in an acute-angled corner, and the swept cavity-floor length would be more nearly equal to the length of the dividing streamline.

The investigation was conducted with the various theoretical analyses of separated flows in mind. It was hoped that the present experimental study would provide comparison data for the theories of Chapman and others, and also provide information useful in the formulation of more involved theoretical treatments. In this respect, it was realized that a regime of laminar, hypersonic cavity flow in which the cavity floor pressure was virtually constant over the section of the cavity upstream of the reattachment region would be of considerable interest. An initial object of the present study was therefore to determine if such a regime existed for laminar hypersonic flows. It is well-known that two stable types of cavity-flow exist -- "open" flows in which the dividing streamline bridges the cavity between separation and reattachment points, and "closed" flows in which the flow reattaches on the cavity floor. In general, the pressure on the cavity floor is not constant in either regime, but there were indications from investigations carried out with transitional, supersonic cavity-flows that within the "open" regime there existed two sub-regions. At low values of cavity length-depth ratio, the pressure

on the cavity floor was usually constant. At higher L/D's, this pattern would gradually change to one with an appreciable pressure gradient on the cavity floor. This change occurred at lower values of L/D than the "critical" value (at which open-closed transition occurred).

In view of these considerations, only open cavity flows were studied in the present investigation. The length-depth ratio of the basic cavity-model was varied over a fairly large range, but was always lower than the critical value.

Besides the cavity length-depth ratio, only one other parameter was varied in the work presented in this report. This was the Reynolds number, which was varied to change the boundary-layer thickness at separation, and also to determine the extent of laminar flow. Transitional flows were not of interest in the present study, but Chapman's work had demonstrated the governing importance of the relative positions of the transition and reattachment points, and it was therefore essential to know the limits of the laminar regime.

For the present work, the free-stream Mach number was kept constant at about 11, giving a cone surface Mach number of about 6.5.

EXPERIMENTAL EQUIPMENT AND TECHNIQUES

All experiments were carried out in the 3 inch helium hypersonic tunnel of the Gas Dynamics Laboratory at Princeton University. This facility is fully described in Ref. 4. Tests were normally made at three levels of stagnation pressure -- 400, 700 and 1000 psia, corresponding to values of unit Reynolds number on the conical model surfaces of 0.59, 0.97 and 1.34×10^6 per inch, respectively. The variation of the centerline Mach number in this range for the contoured nozzle used is shown in Figure 2.

For the present investigation, 10 pressure models were made. One of these was a 20° total-angle cone used for normalization. All cavity-models were based on this geometry. Eight models incorporated cavities of the same general shape, with varying values of length and depth. The remaining model was designed with a cavity formed from a single circular arc. The models are sketched in Figure 1.

All models were made of brass and were instrumented with pressure leads made from copper to avoid outgassing. All models were machined with a nose diameter of 0.005 inches to ensure that the hypersonic nose effect would be constant. Each model carried 4 pressure taps spaced 90° apart at a single axial station on the conical surface downstream of the cavity position. These were used to align the models while the tunnel was running.

The method of alignment was checked by deliberately misaligning several of the models during test runs, and noting the changes which occurred in the pressures. For most of the measurement points, including the alignment station, the pressure varied slowly and continuously with angle of alignment, and it was concluded that the aligning method was completely satisfactory. The only region in which the pressure level changed greatly with small changes in model alignment was in the immediate vicinity of the reattachment point. For this reason, in the results which follow, it is felt that the measurements made near reattachment should be taken as giving the position and extent of the reattachment pressure rise rather than a quantitative measure of the actual pressures. With this reservation, the repeatability of the pressure measurements was very good.

Pressure measurements were taken on conventional oil manometers, except for particularly high pressures, where mercury manometers were used.

Schlieren photographs were taken using a two-mirror system with a one microsecond spark light source. A "Fastax" movie camera running at up to 8,000 frames per second was used to check the steadiness of the flow.

RESULTS OF EXPERIMENTS

PURE-CONE PRESSURE DISTRIBUTION

The pressure measurements on the pure-cone model were checked by normalising them by the local static pressure in the tunnel at the particular stagnation pressure of each test. The results of this are given in Figure 3, and are compared with the theoretical inviscid values from Ref. 5, for two bracketing values of the tunnel free-stream Mach number. It can be seen that the hypersonic nose effect is negligible for the present models, since the measured pressure on the cone is constant with axial distance from the nose, once allowance has been made for tunnel variations.

In normalising the cavity-model pressure results, a mean of several tests on the basic cone was used at each stagnation pressure. The experimental spread of the cone data around this mean was found to be $\pm 1\frac{1}{2}\%$ at most.

CAVITY-MODEL RESULTS

The pressure results on the cavity models were normalised by the cone pressure at the particular values of axial station and stagnation pressure of each data point. The results are presented in terms of a distance parameter defined as follows:

<u>Position</u>	<u>Parameter</u>	<u>Definition</u>
Upstream of separation shoulder	\bar{x}/δ_S	$\bar{x} = x_S - x$
Within cavity	\bar{x}/L	$\bar{x} = x_R - x$
Downstream of reattachment shoulder	\bar{x}/L	$\bar{x} = x - x_R$

For convenience, the results from the regions upstream of, within, and downstream of the cavity on each model will be described separately.

Upstream of Separation Shoulder

These results are presented in Figure 4. In the second part of the present report, recovery factor measurements on the basic cone will be presented which show that the boundary layer at separation was always laminar throughout the present tests. From Figure 4, it is seen that the disturbance due to the presence of the cavity on each model is propagated upstream about 10 to 15 boundary-layer thicknesses. This upstream influence is strongest at $p_o = 400$ psia and weakest at $p_o = 1000$ psia, as would be expected from the relative thicknesses of the boundary-layer in each case.

Pressure Distribution within Cavity

These results are presented in Figures 5 through 13. Results are given for each cavity model in turn, each set containing measurements at $p_o = 400, 700$ and 1000 psia. A detailed discussion of these results will be deferred until later, when the effect of cavity length-depth ratio is described.

Downstream of Reattachment Shoulder

These results are given in Figures 14, 15 and 16 for the three levels of stagnation pressure used. For all cavity models, the pressure decayed quickly in the downstream direction. The pressure level dropped to the cone value in about one cavity length or less for all models and stagnation pressures. For comparison purposes, a decay curve corresponding to the inverse first power of \bar{x}/L is shown on each figure. (Actually,

the equation

$$\frac{P}{P_{\text{cone}}} - 0.975 = \frac{0.036}{\bar{x}/L} \quad . \quad)$$

In all cases tested, the pressure on the surfaces downstream of reattachment eventually dropped to a value about 3% below the mean cone value.

Transition from the Laminar Regime

In a hypersonic tunnel such as the present facility, in which test-section density is rather low, it is not easy to detect transition because of the reduced effectiveness of conventional optical techniques. In the present investigation, information obtained from several techniques was used to determine the limits of the laminar regime. In this section, evidence of transition on the cavity models obtained from schlieren photographs, and from the measured pressure distributions will be presented. The results of the recovery-factor and heat-transfer tests yield further information, and this is presented in Part II of the present report. It will be observed at this point that the Reynolds number for natural transition on the pure cone was determined from recovery factor measurements to be about 2×10^6 . (based on length from the nose along the slant side of the cone, and on fluid properties at the edge of the boundary layer).

A series of schlieren photographs of one of the long-cavity models is presented in Figure 17. Plates were taken at 100 psia intervals in stagnation pressure. A definite change in the character of the lines indicating the edge of the mixing layer and the downstream boundary layer can be detected as the stagnation pressure rises. In the picture taken

at $p_0 = 1000$ psia, transition apparently occurs somewhere in the middle of the cavity.

A method of detecting transition using measurements of the pressure in the reattachment corner of a separated flow is used by Chapman and his co-workers. In Ref. 6, Chapman demonstrates that the pressure just before reattachment rises sharply with the appearance of transition inside the separated region. In Ref. 7, Larson and Keating use this as an indicator of transition for cavity flows. It is probable that the pressure rise occurs in cavity flows as a result of the increased kinetic impact pressure of the turbulent mixing profile. In Figure 18, the pressure at the last measuring orifice in the cavity before the reattachment shoulder of the model with $L = 1-1/4$ inches and $D = 3/32$ inches in the present series is plotted as a function of Reynolds number based on the length to the reattachment shoulder. The sharp pressure rise which occurs as the Reynolds number increases is well marked.

From the above results, and from the heat-transfer and recovery factor information, it was concluded that the cavity flows in the present investigation were laminar up to a reattachment Reynolds number of about 2×10^6 (characteristic length taken as $L + L_1$). Since this value is the same as the transition Reynolds number on the cone, it may be said that the laminar separated layer was as stable as the attached laminar boundary layer for the present tests, within the level of experimental uncertainty.

It should be realized that transition will occur at rather different Reynolds numbers on models with different thermal characteristics, as is well brought out by the work of Larson and Keating in Ref. 7. However, the intention in the present investigation was not to locate

transition exactly, but simply to define a regime which was always laminar.

Steadiness of the Cavity Flows

High-speed movie films were taken of the flow over several of the cavity models using a "Fastax" camera coupled to the schlieren system. Film speeds up to 8,000 frames per second were used, and both laminar and transitional flows were studied. In the case of the laminar cavity flows, no unsteadiness could be detected. However, there were indications of unsteadiness in the transitional flows. This appeared to take the form of fluctuation of the position of the transition point, wave radiation from the rear of the cavity, and variation in the appearance of the weak shockwave as the flow reattached.

The "Fastax" films yielded pictures which were of much poorer quality than the conventional spark schlieren photographs. This was due to the small frame size necessary (16 mm), the lens system of the camera and the relative weakness of the continuous light source used with the movie camera. In view of these limitations, another method was tried. This involved taking a number of spark schlieren photographs at random time intervals during a single run. These photographs were then magnified 20 times on an optical comparator, and tracings made of the position of the shockwaves and dividing streamlines for each plate photograph. This method would detect any oscillatory unsteadiness with a frequency less than 10^6 per second, since the one-microsecond spark photographs would show different parts of the cycle.

It was found that the maximum fluctuation of the dividing streamline which could be detected in laminar cavity-flow was about 3.8% of the

cavity depth in the direction normal to the model surface. The maximum bow shockwave fluctuation was about half this value. Photographs taken of transitional cavity-flow showed the same indications of unsteadiness which had been seen in the movie films.

No fluctuations in pressure level were ever observed on the manometers in either the laminar or transitional regime during the pressure tests.

It was concluded from the above results that the laminar cavity-flows were steady within the limits of the detection techniques, and that the transitional flows were unsteady. All tests indicated that if any unsteadiness were present in the laminar cavity flows, it was not of sufficient magnitude to affect the quantities being measured.

Variation of the Cavity Pressure Distributions with Length-Depth Ratio

In cavity-flows, there are four characteristic lengths which define a particular problem. These are the boundary-layer thickness at separation, the length and depth of the cavity, and the critical cavity length. The particular combination of these in non-dimensional form which correlates experimental results has apparently not yet been found. Most investigators use the cavity length-depth ratio in presenting results. Charwat et al, (Ref. 8) claim that L/L_{Cr} is the characteristic parameter, but they present their results in terms of L/D and δ_s/D . In the present investigation, the length-depth ratio has been found to be a useful parameter, although it certainly does not provide a complete picture.

An examination of the cavity results in Figures 5 through 13 shows that at low values of L/D , the pressure is virtually constant

with \bar{x}/L for about the first 90% of the cavity. After this station, the reattachment pressure rise sets in. At higher values of L/D , a definite pressure gradient appears on the cavity floor. In virtually all cases, the pressure on the cavity floor is lower than cone pressure. The dividing streamline normally starts with a slight inclination inwards towards the model axis (less than 1°). The only case for which the dividing streamline bent outwards at separation was the $p_0 = 1000$ psia test on the $L = 1\text{-}1/4$ inches, $D = 1/8$ inch model (Figure 11). This test was in the transitional regime. Diagrammatic sketches of the flow patterns in these various regimes are given in Figure 19.

In Figure 20, the cavity floor pressures at the beginning and end of the straight section are plotted for each model against length-depth ratio. The stagnation pressure for these results was 400 psia, and at this pressure all cavity flows were laminar. The existence of a regime of constant floor pressure is clearly evident. When the length-depth ratio rises to about $7 \sim 10$, a pressure gradient appears on the cavity floor. It should be emphasized that all results presented are for "open" cavity flows, even for the case of $L/D = 20$. Schlieren photographs of a model with $L/D = 40$ showed that this model was in the "closed" regime. Thus, for laminar cavity flows of the present type

$$20 < \frac{L_{Cr}}{D} < 40 .$$

The pressure distribution on the model incorporating a cavity formed from a single circular arc ($L/D = 5$) was found to be virtually the same as the other models in the short-deep range, although the recompression pressure rise set in a little further upstream (Figure 8).

The effect of decreasing the value of δ_s/D for any particular value of L/D was to raise the cavity floor pressure. This effect becomes stronger with increasing L/D . In the present experiments, the theoretical value of δ_s (Ref. 9) was as follows:

<u>p_o (psia)</u>	<u>δ_s (inches)</u>
400	0.0225
700	0.0176
1000	0.0151

As a result, the range of δ_s/D investigated was from 0.12 to 0.36.

COMPARISON WITH OTHER INVESTIGATIONS

The present investigation is concerned with laminar, open cavity flows at hypersonic Mach numbers. In a search of the available literature, very little work on laminar cavity flows was found. In addition, the cone-cavity geometry used in the present work does not appear to have been investigated before. However, in one respect at least an interesting comparison can be made between the present results and the work of other investigators.

As was mentioned previously, one of the objects of the present study was to determine if a regime of laminar cavity flows existed which was characterized by constant floor pressure over most of the cavity span. The results of the pressure tests show that such a regime exists for L/D less than about 7. The work of Johannesen in Ref. 10, McDearmon in Ref. 11, and Charwat et al in Ref. 8, shows that this "short-deep" regime exists in transitional flow at supersonic Mach numbers. The division of cavity flows into three regimes (deep open flows, shallow open flows and closed flows),

rather than two (open and closed) is particularly well brought out by McDearmon. Johannesen had laminar flow for his shortest cavities, and believed that the change from constant floor-pressure cavity flows to shallow open flows was caused by transition appearing in the separated-flow region. Charwat et al disagree, and say that the change is brought about by the appearance of a weak oblique shock rooted in the shear layer which is neither caused by nor dependent on transition from the laminar regime. Instead, it is due to a deflection of the external stream which is a part of the recompression mechanism. The present results are also in conflict with Johannesen's explanation, since both forms of open cavity-flow were found even when the flows were laminar throughout (Figure 20).

The changeover from open to closed flows in the laminar regime was not determined exactly in the present investigation since closed flows were not of interest. However, the critical value of L/D was found to lie between 20 and 40. The only comparisons which can be made are Larson's value of 30 in Ref. 7, and Kavanau's value of about 25 in Ref. 12. No other measurements are known to the present author. It appears that the critical length-depth ratio is not strongly dependent on Mach number.

The pressure levels encountered in the present investigation are similar to those of other workers, ranging from a low of $p/p_c = 0.6$ in the cavity, to about $p/p_c = 2$ at reattachment. We can obtain some idea of the maximum reattachment pressure in laminar flow from Chapman's work in Ref. 6. Assuming laminar, steady, two-dimensional cavity flow, with isentropic compression along the dividing streamline and zero initial boundary layer thickness, with a Prandtl number of 1 and with "dead-air" temperature equal to outer stream total temperature, Chapman's analysis gives the following equation for the reattachment pressure ratio:

$$\frac{p_R}{p_e} = \left[\frac{1 + \frac{\gamma-1}{2} M_e^2}{1 + \frac{\gamma-1}{2} M_e^2 (1-u_*^2)} \right]^{\frac{\gamma}{\gamma-1}}$$

In which $u_* = 0.587$.

For the present work, $\gamma = 5/3$, $M_e \sim 6.5$ and thus

$$\frac{p_R}{p_e} = 7.3$$

This should be an upper limit on the pressure at the reattachment shoulder in laminar flow. Any entropy rises in the recompression process will result in a drop in the pressure at reattachment. Also, any initial boundary layer at separation will result in a lower value of u_* , with a consequent drop in kinetic energy impact pressure. The pressure measurements made very near the reattachment shoulder in the laminar flow studies of the present work never gave values of p/p_e greater than about 1.4. Despite the fact that these measurements cannot be very accurate, and in addition must be less than p_R/p_e , the low value of the ratio indicates that the effect of finite initial boundary layer may be very important. (It is unlikely that entropy changes in the recompression process will be significant. When shockwaves at reattachment were visible at all in schlieren photographs, they were always very weak.)

CONCLUDING REMARKS

The present investigation consists of measurements of the pressure distribution on a set of annular cavities on a 20° cone. The cavity flows

were "open", the flows were either laminar or transitional, and the free stream Mach number was about 11.2. (cone surface Mach number 6.5).

In the laminar regime, it was possible to distinguish between two regimes of open cavity flow, with the following characteristics:

1. Deep open flows ($L/D < 7$)

Pressure distribution insensitive to changes of L/D . Cavity floor pressure constant over first 90% of cavity. Cavity floor pressure about 10-15% lower than basic cone pressure. Recompression confined to small region near the reattachment point.

2. Shallow open flows ($7 < L/D < L_{Cr}/D$)

Pressure distribution insensitive to L/D . Dividing streamline concave out. Recompression occurs along dividing streamline as well as in reattachment region. Significant pressure gradients on cavity floor.

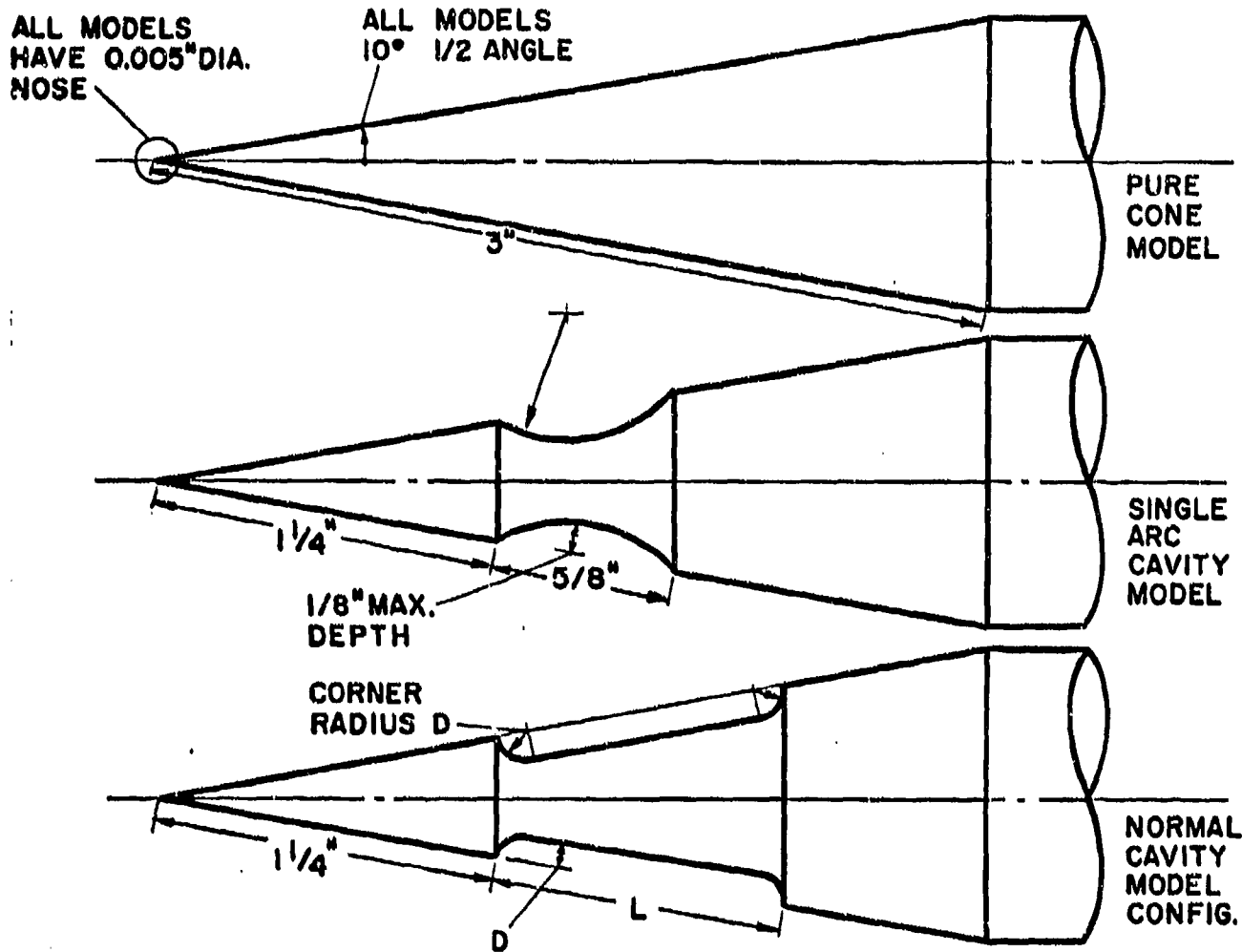
The division of the cavity flows according to the above result, and including a distinction between laminar and transitional flows, is shown diagrammatically in Figure 21. In this figure, the various models tested are shown entered in the appropriate region for each stagnation pressure. (Each model is identified by the length and depth of the cavity, as L inches \times D inches.) In the case of the deep, 5/8 inches long-cavity models at $p_0 \sim 1000$ psia, their entry in the transitional flow regime is based on recovery factor and heat-transfer measurements, since these models were too close to the borderline for reattachment pressure measurements to be conclusive.

The region of deep, laminar, open cavities is shown shaded, and is the primary regime of interest in the present program. In Figure 22, the cavity pressure distributions for all the tests in this regime are superimposed.

From this figure it can be seen that the pressure distribution is virtually constant for a quite wide range of cavity length-depth ratio and boundary-layer thickness at separation.

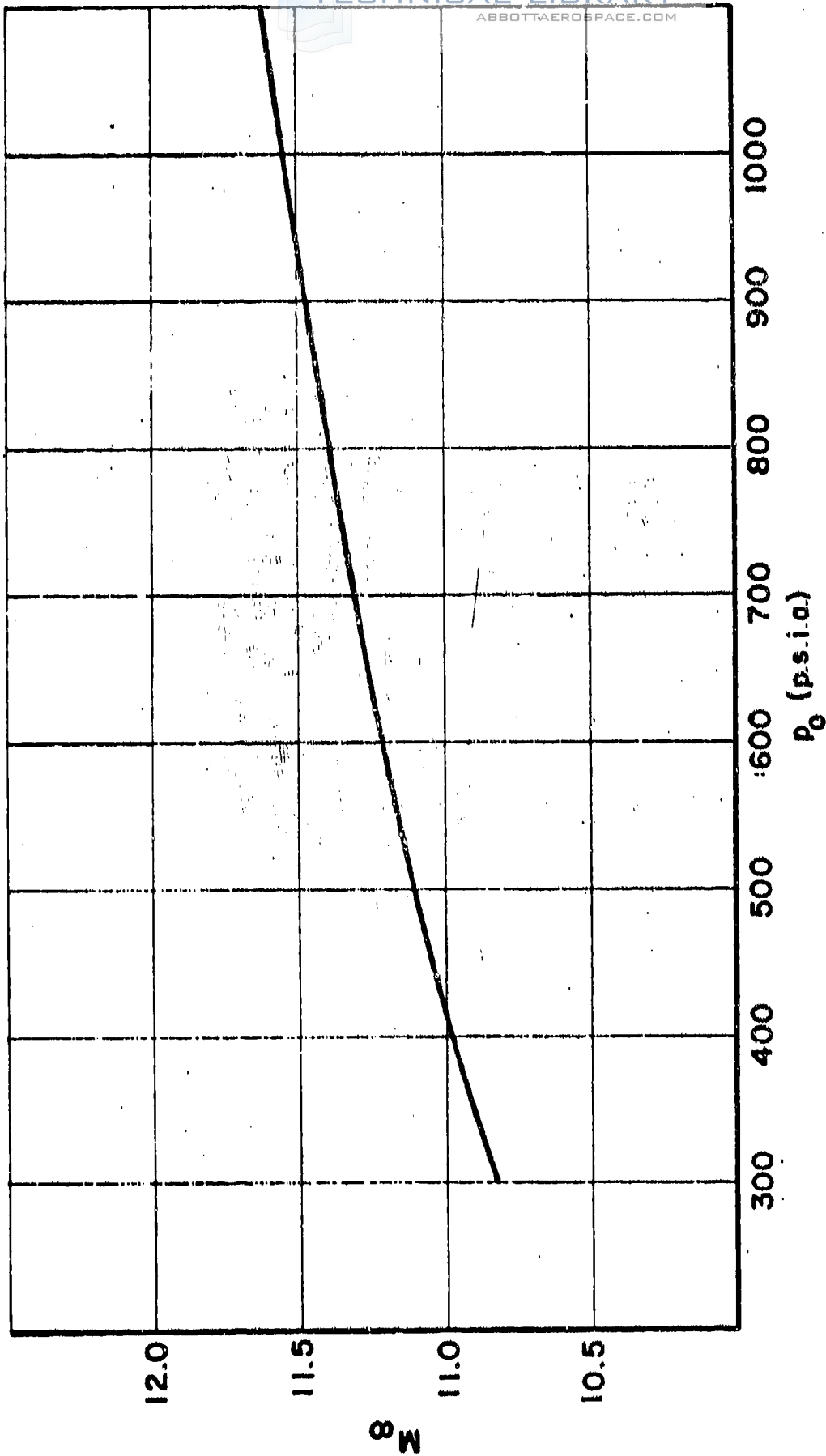
REFERENCES

1. Chapman, D. R.; Kuehn, D. M. and Larson, H. K.: Preliminary Report on a Study of Separated Flows in Supersonic and Subsonic Streams. NACA RM A55L14, 1956.
2. Chapman, D. R.: A Theoretical Analysis of Heat Transfer in Regions of Separated Flow. NACA TN 3792, 1956.
3. Larson, H. K.: Heat Transfer in Separated Flows. IAS Report 59-37, January 1959.
4. Bogdonoff, S. M. and Hammitt, A. G.: The Princeton Helium Hypersonic Tunnel and Preliminary Results Above $M = 11$. PUAED 260, June 1954; also published as WADC TN 54-124.
5. Henderson, A. and Braswell, D. O.: Charts for Conical and Two-dimensional Oblique-shock flow Parameters in Helium at Mach Numbers from About 1 to 100. NASA TN D-819, June 1961.
6. Chapman, D. R.; Kuehn, D. M. and Larson, H. K.: Investigation of Separated Flows in Supersonic and Subsonic Streams with Emphasis on the Effect of Transition. NACA Report 1356, 1958 (supercedes NACA TN 3869).
7. Larson, H. K. and Keating, S. J.: Transition Reynolds Numbers of Separated Flows at Supersonic Speeds. NASA TN D-349, December 1960.
8. Charwat, A. F.; Dewey, C. F.; Roos, J. N. and Hitz, J. A.: An Investigation of Separated Flows. JASS, June and July 1961.
9. Nicoll, K. M.: Investigation of the Laminar Boundary Layer on a Flat Plate in Helium Using the Crocco Method. PUAED 590, December 1961; also published as ARL 62-345.
10. Johannesen, N. H.: Experiments on Supersonic Flow Past Bodies of Revolution with Annular Gaps of Rectangular Section. Phil. Mag. [7], V46 No. 372, pp. 31-39, January 1955.
11. McDearmon, R. W.: Investigation of the Flow in a Rectangular Cavity in a Flat Plate at a Mach Number of 3.55. NASA TN D-523, September 1960.
12. Kavanau, L. L.: Results of Some Base Pressure Experiments at Intermediate Reynolds Numbers with $M = 2.84$. JAS, V 21, No. 4, p. 257, April 1954.

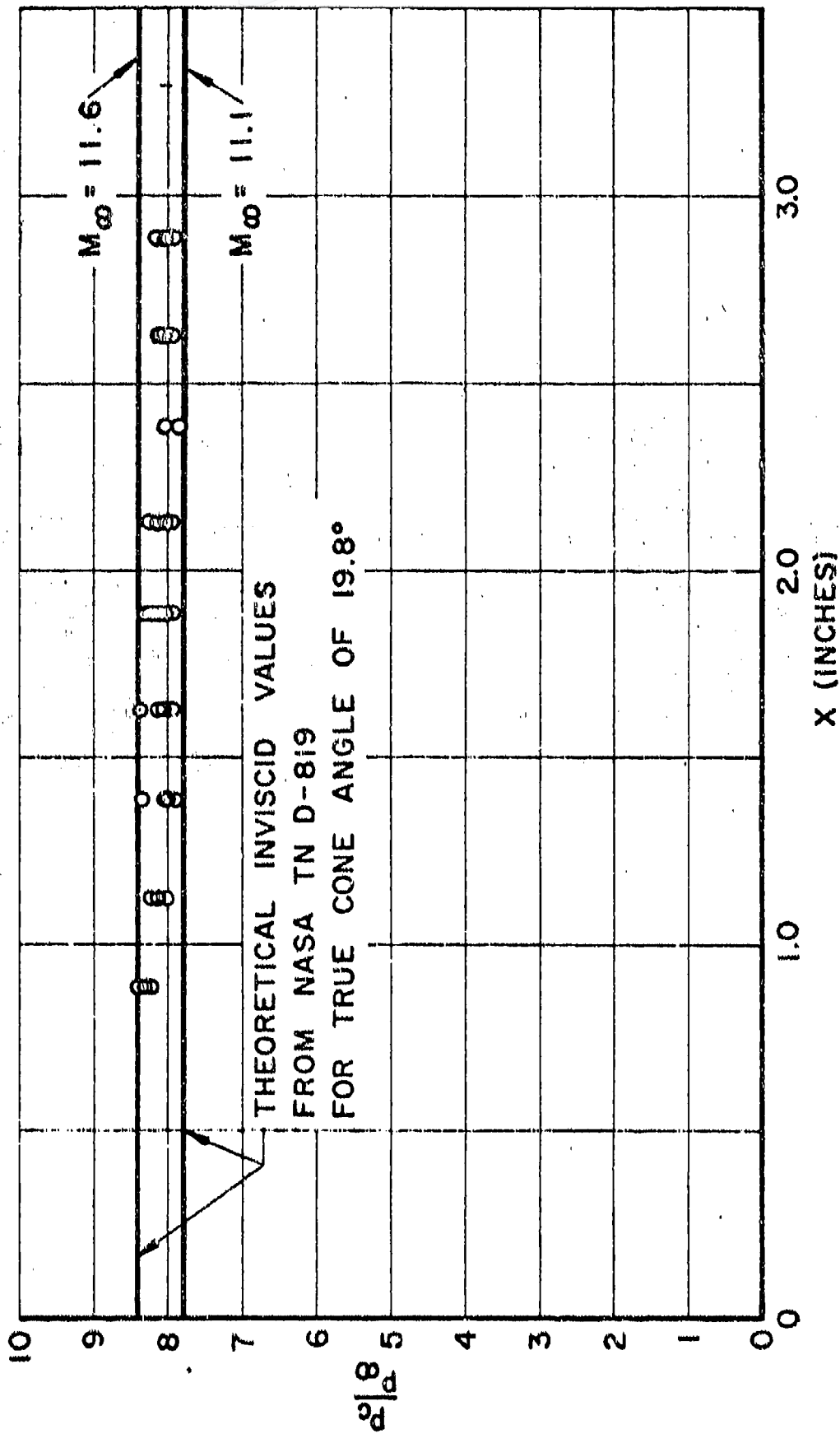


	L"	D"	L/D
DIMENSIONS FOR SET OF EIGHT CAVITY MODELS WITH GEOMETRY AS IN LOWEST SKETCH ABOVE.	5/16	1/8	2.5
	"	3/32	3.33
	5/8	1/8	5.0
	"	3/32	6.67
	"	1/16	10.0
	1 1/4	1/8	10.0
	"	3/32	13.33
	"	1/16	20.0

GEOMETRY OF PRESSURE MODELS
 (ALL AXI-SYMETRIC)

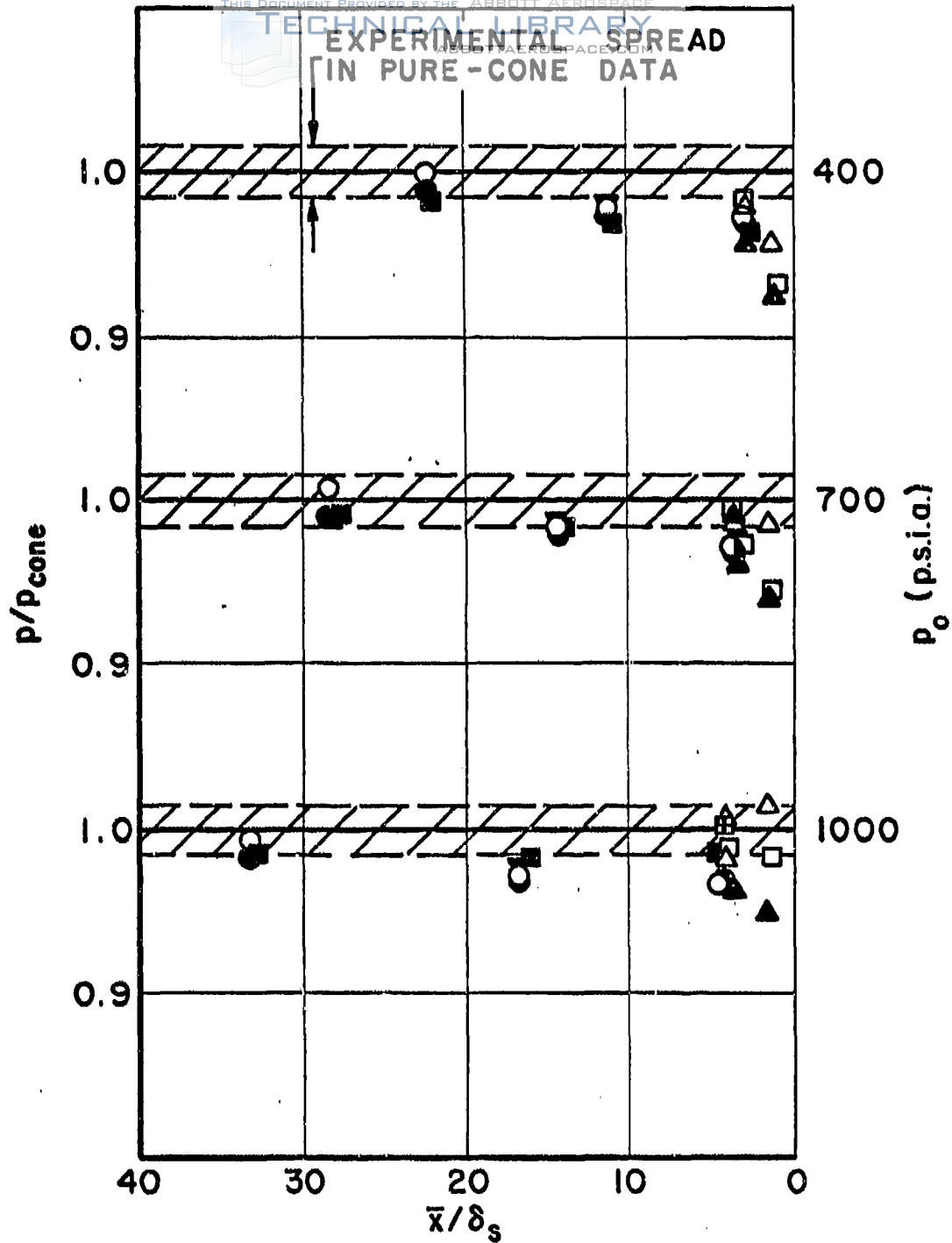


FREE STREAM MACH NUMBER IN TUNNEL AT NOSE OF MODEL



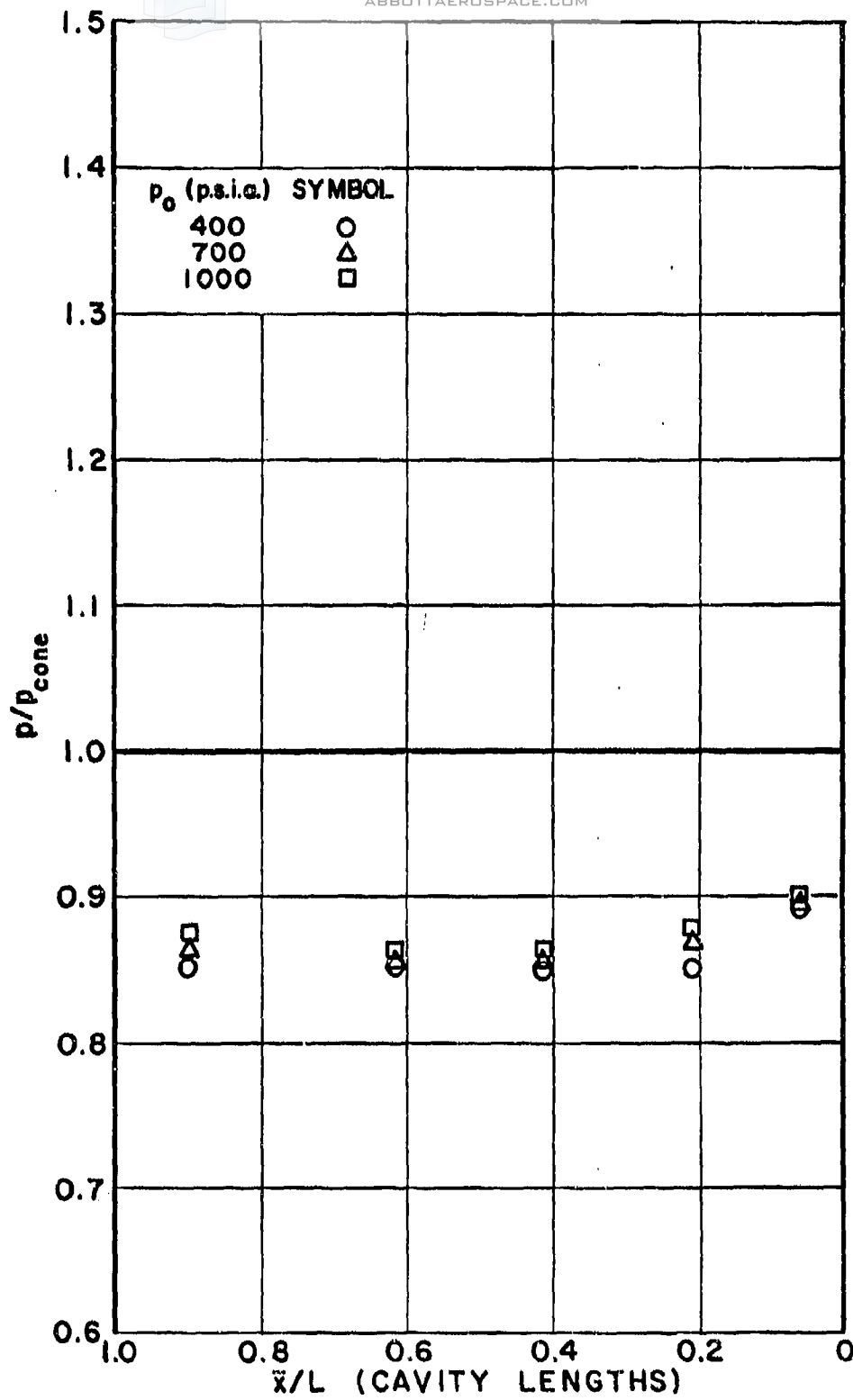
EXPERIMENTAL PRESSURE RESULTS
ON 20° TOTAL-ANGLE CONE

TECHNICAL LIBRARY
 EXPERIMENTAL SPREAD
 IN PURE-CONE DATA



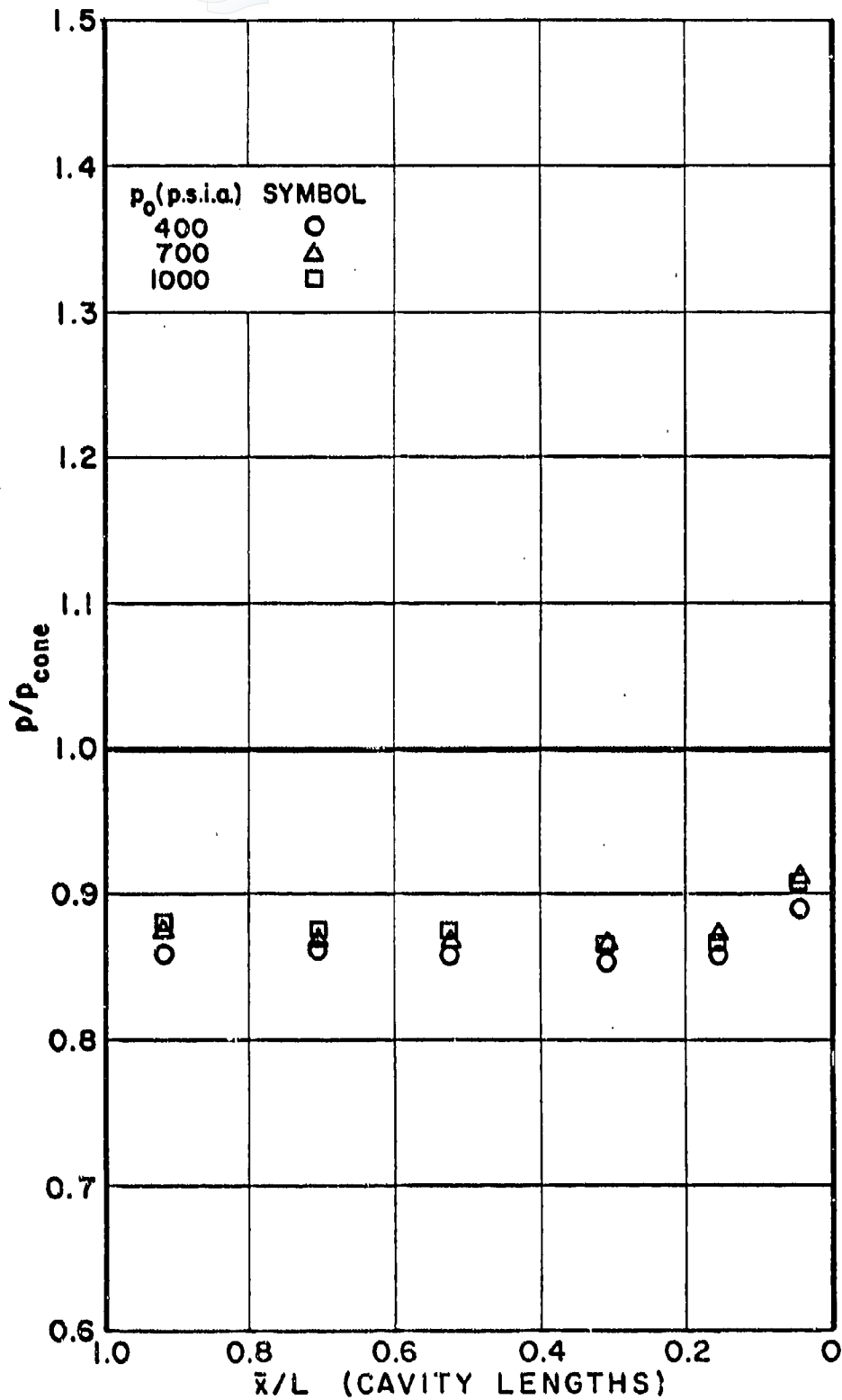
CAVITY	L"	5/16	5/16	5/8	5/8	5/8	5/8	1/4	1/4	1/4
DIMENSIONS.	D"	1/8	3/32	1/8	1/8	3/32	1/16	1/8	3/32	1/16
SYMBOL.		●	○	▲	▼	△	▲	■	□	▣
					↑					
					SINGLE ARC					

PRESSURE DISTRIBUTION UPSTREAM
 OF SEPARATION SHOULDER

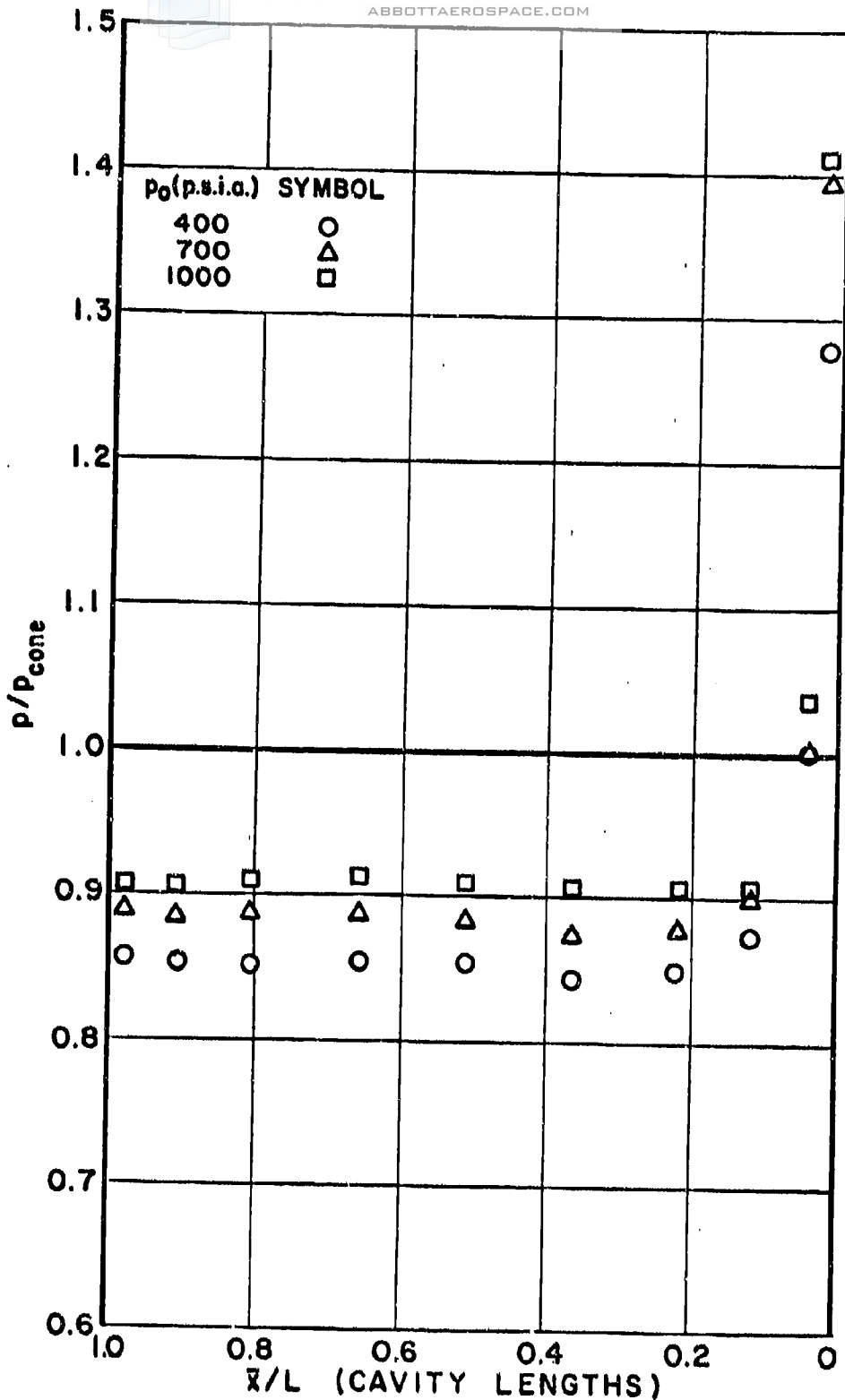


PRESSURE DISTRIBUTION WITHIN CAVITY
 $L = 5/16''$ $D = 1/8''$

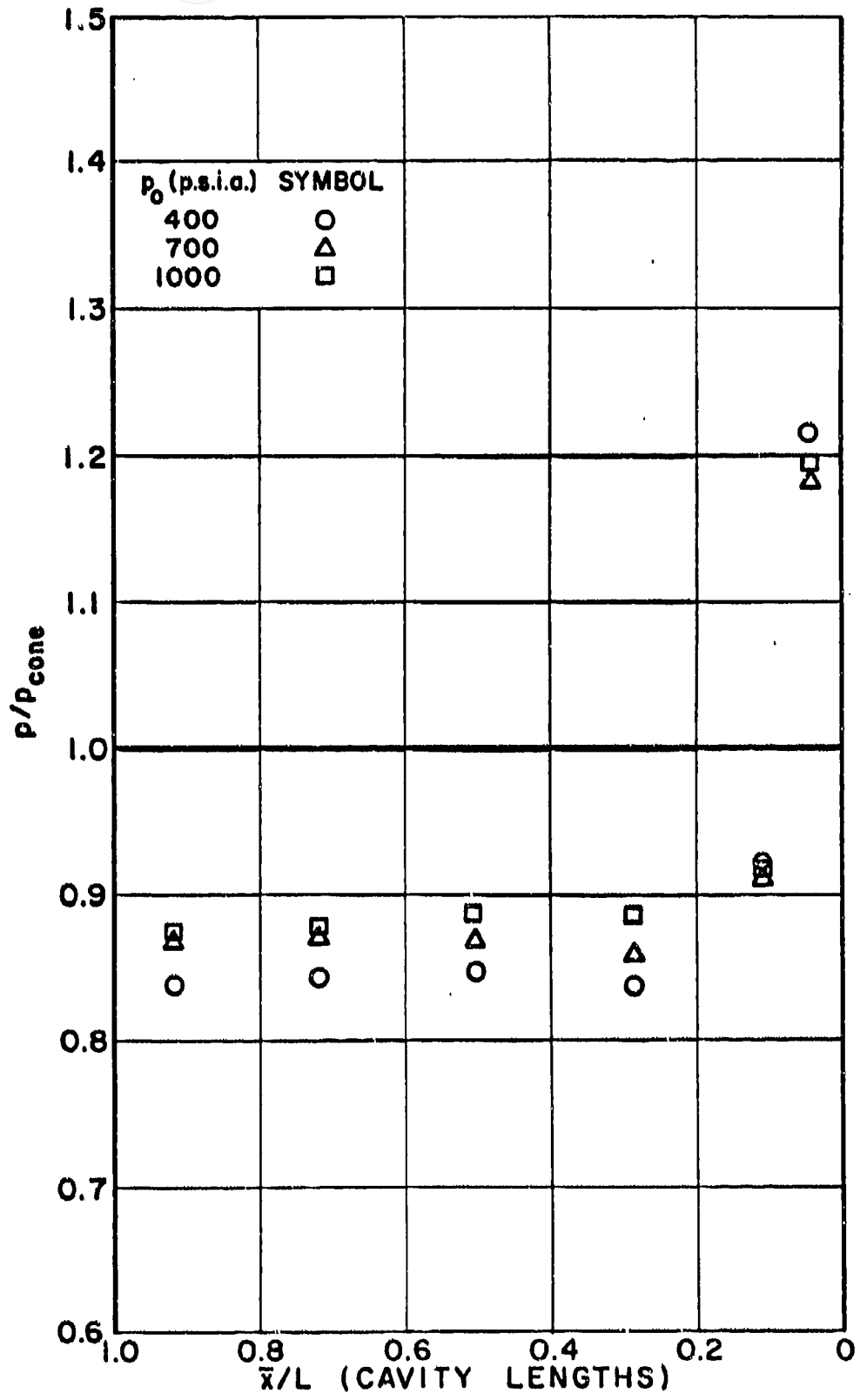
XII B3-5
Figure 5.



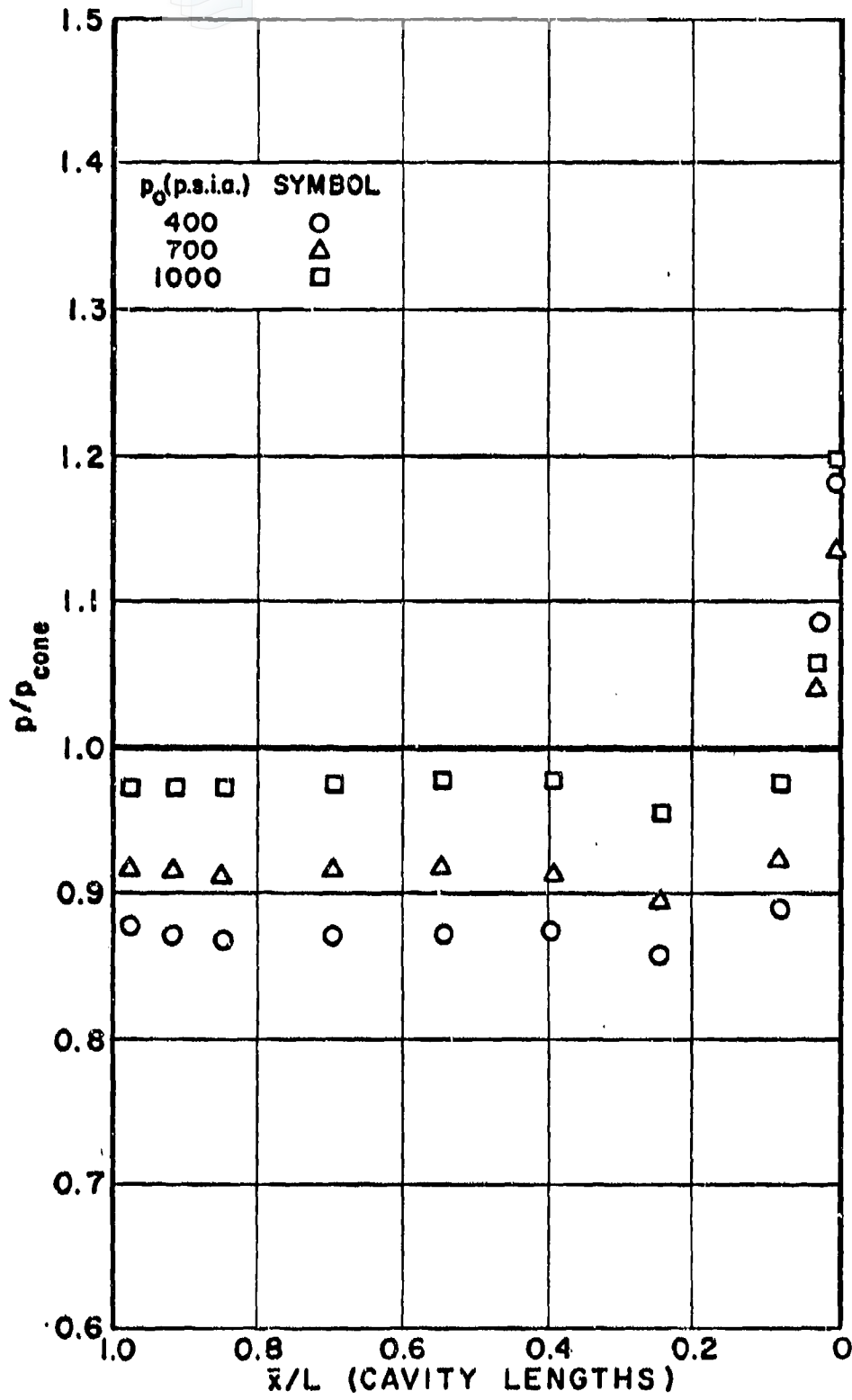
PRESSURE DISTRIBUTION WITHIN CAVITY
 $L = 5/16''$ $D = 3/32''$



PRESSURE DISTRIBUTION WITHIN CAVITY
 $L = 5/8''$ $D = 1/8''$

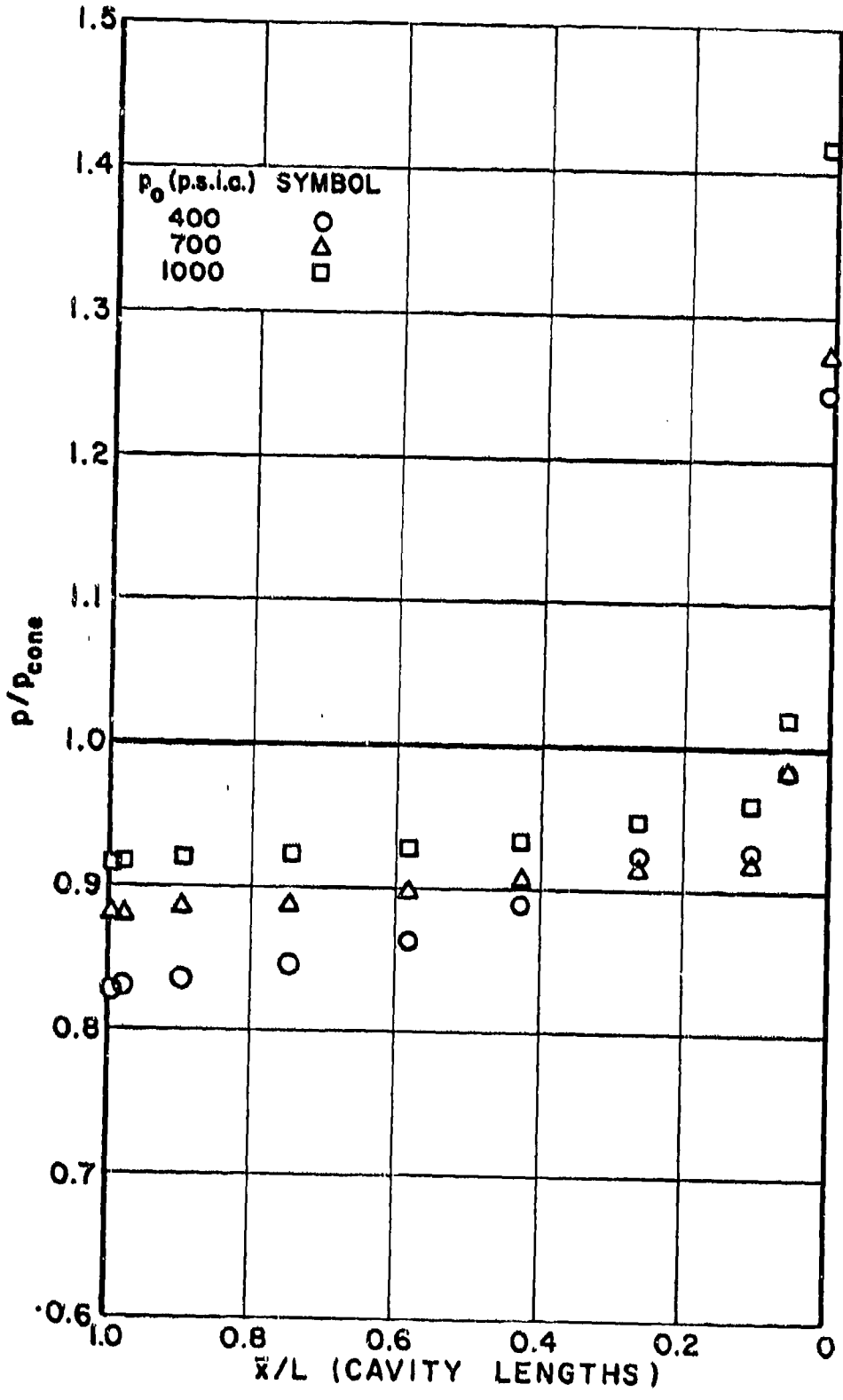


PRESSURE DISTRIBUTION WITHIN CAVITY
 L=5/8" D=1/8" , SINGLE-ARC

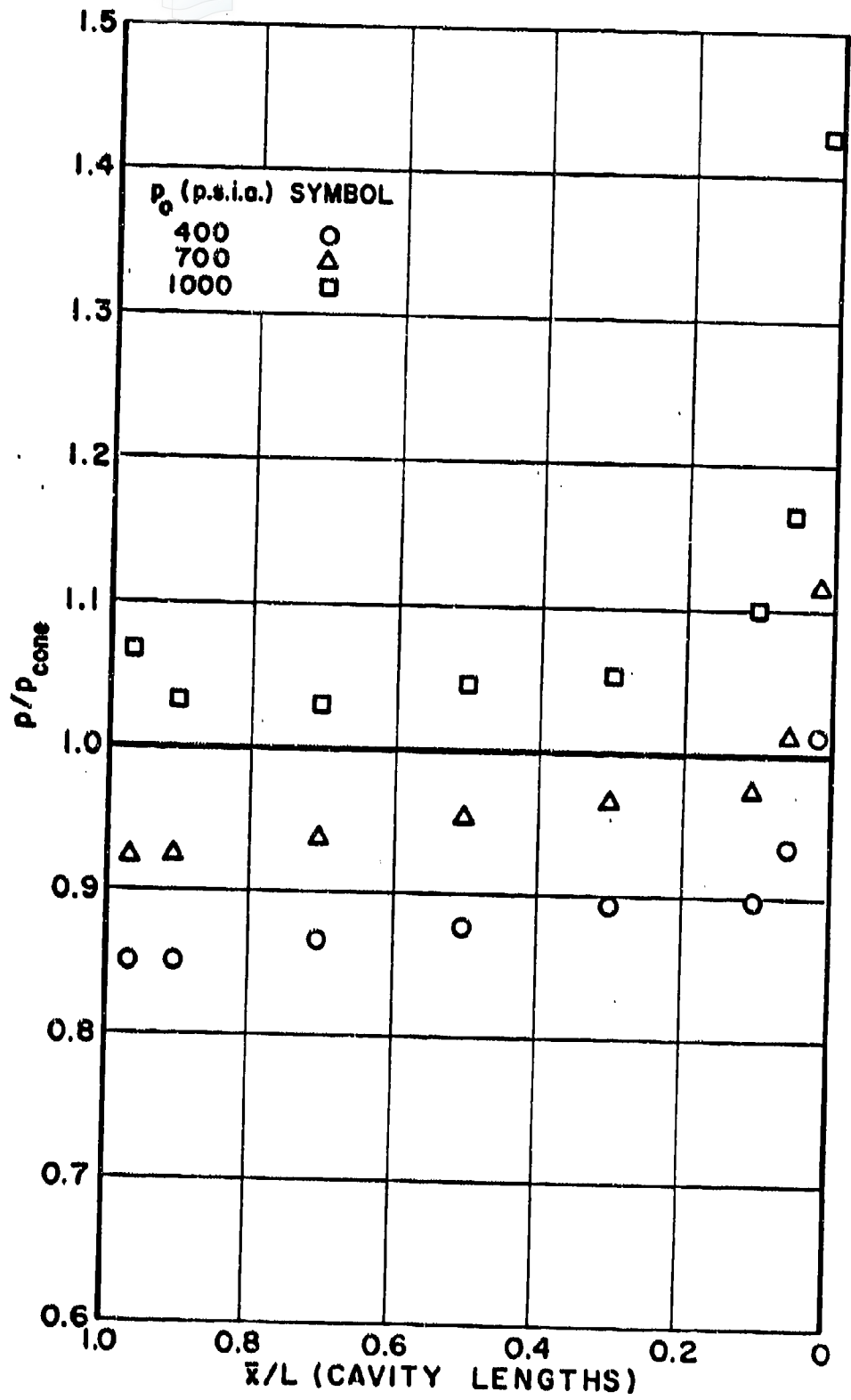


PRESSURE DISTRIBUTION WITHIN CAVITY
 $L = 5/8''$ $D = 3/32''$

XII B3-9
 Figure 9.

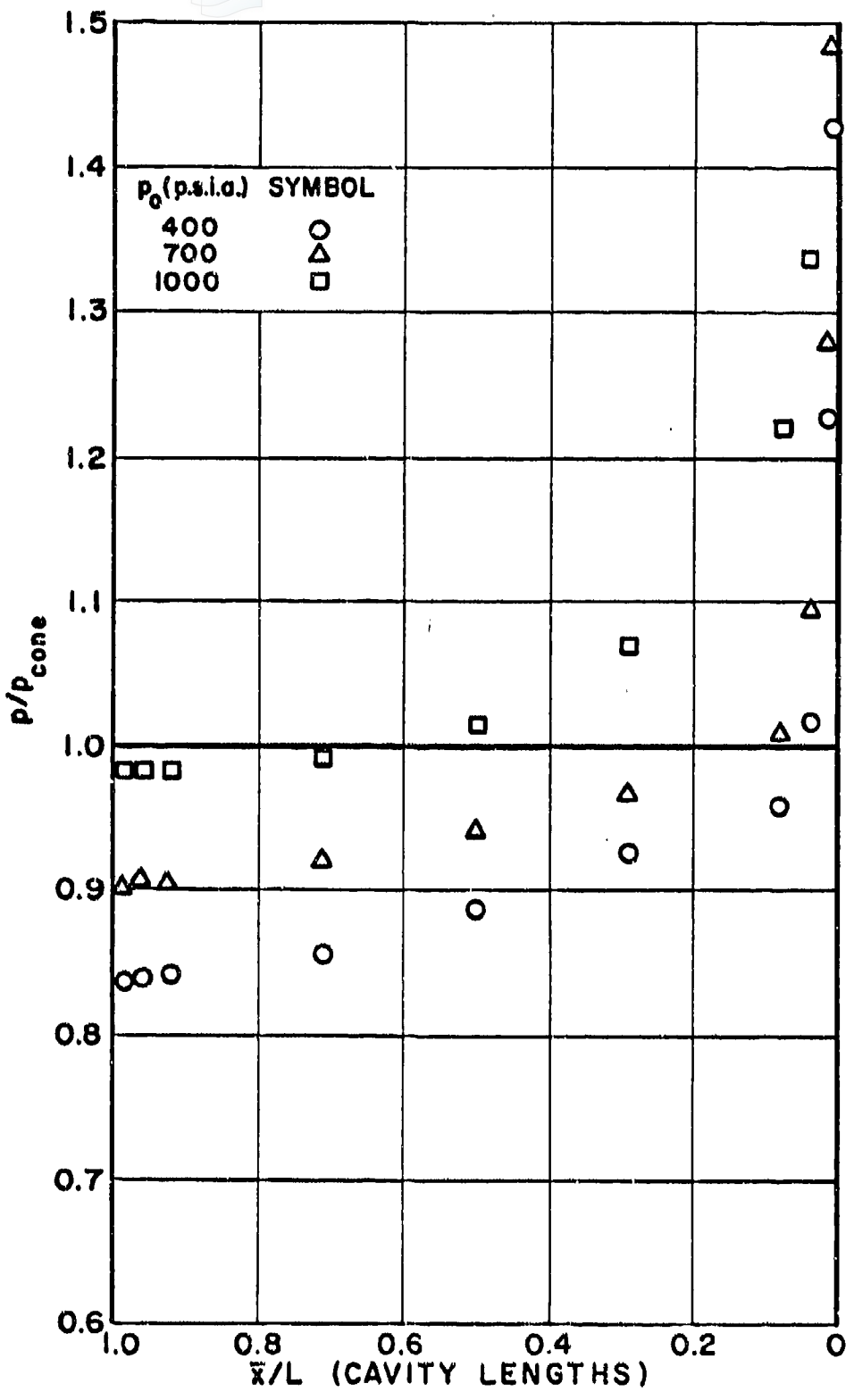


PRESSURE DISTRIBUTION WITHIN CAVITY
 $L = 5/8''$ $D = 1/16''$



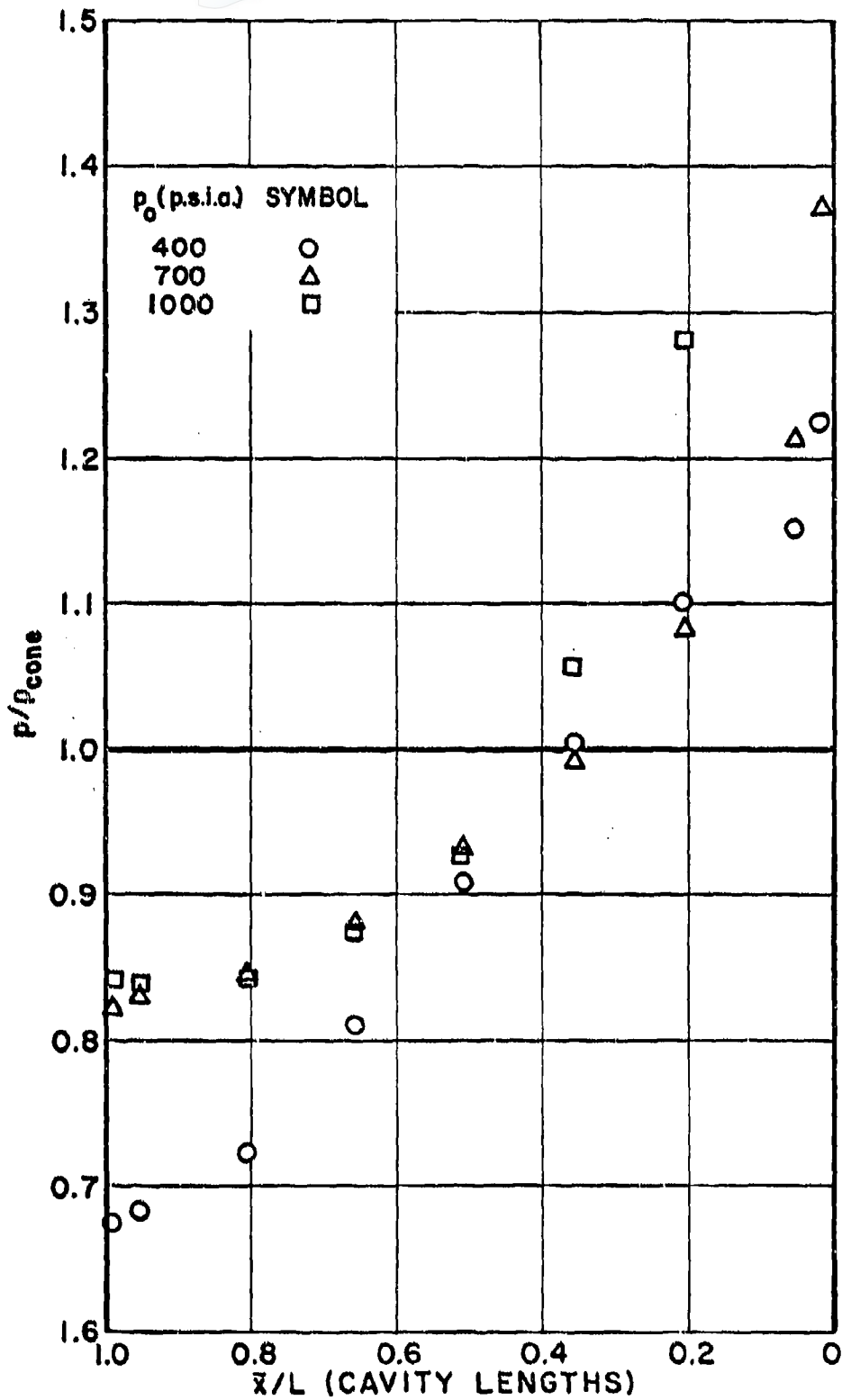
PRESSURE DISTRIBUTION WITHIN CAVITY
 $L = 1\frac{1}{4}"$ $D = 1/8"$

XII B3-11
 Figure 11.



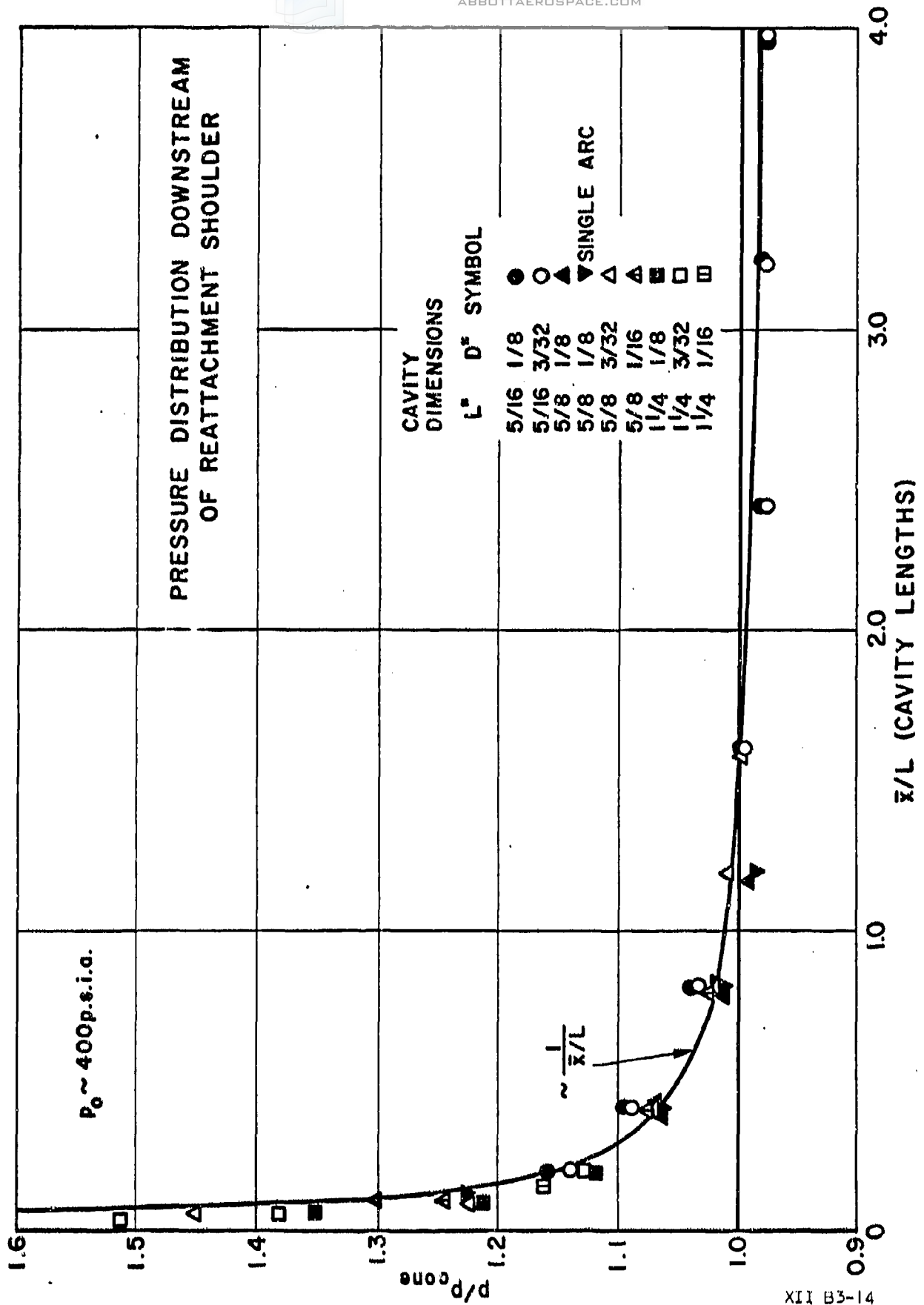
PRESSURE DISTRIBUTION WITHIN CAVITY
 $L = 1\frac{1}{4}''$ $D = 3/32''$

XII B3-12
 Figure 12.

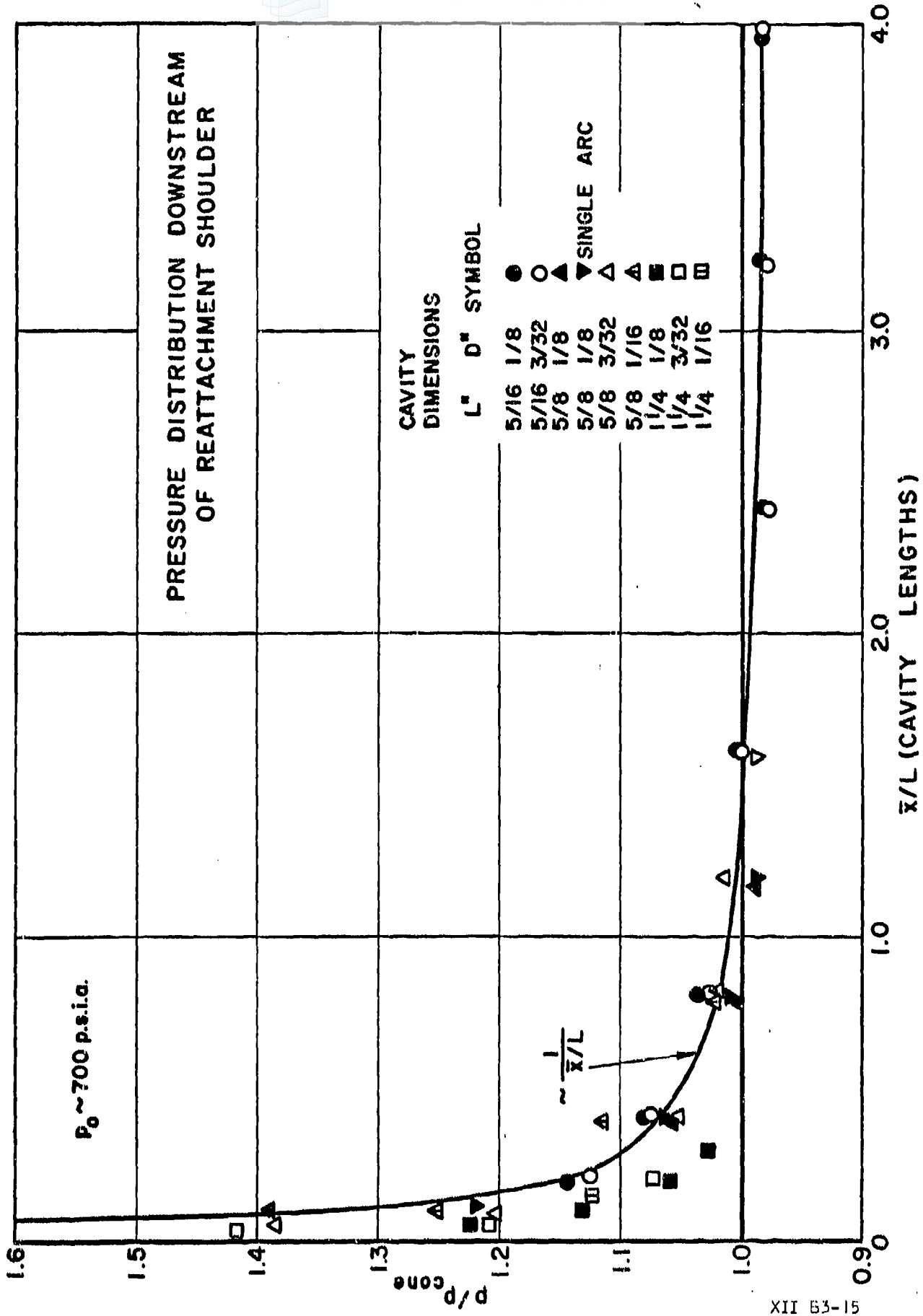


PRESSURE DISTRIBUTION WITHIN CAVITY
 $L = 1/4''$ $D = 1/16''$

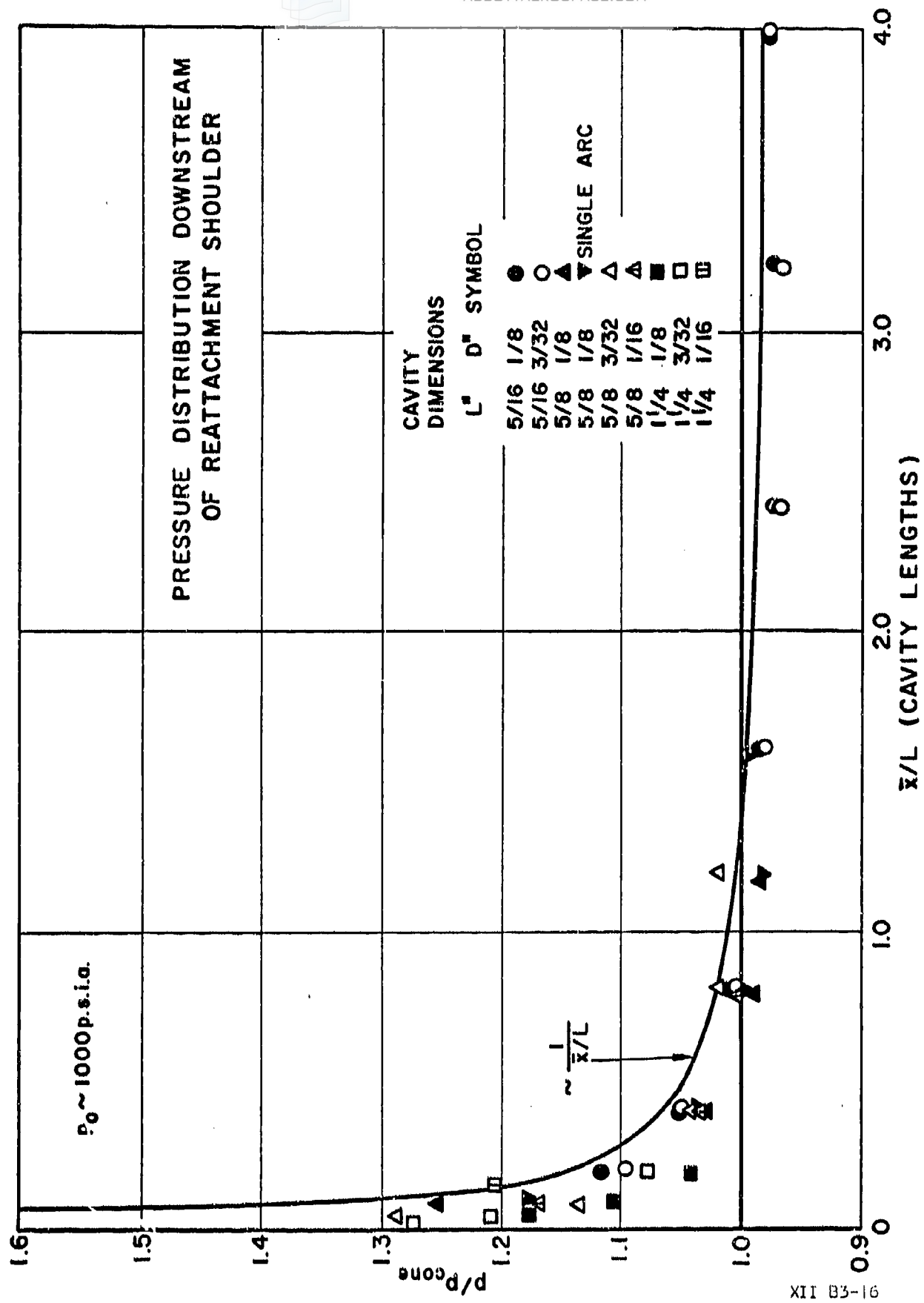
XII B3-13
 Figure 13.



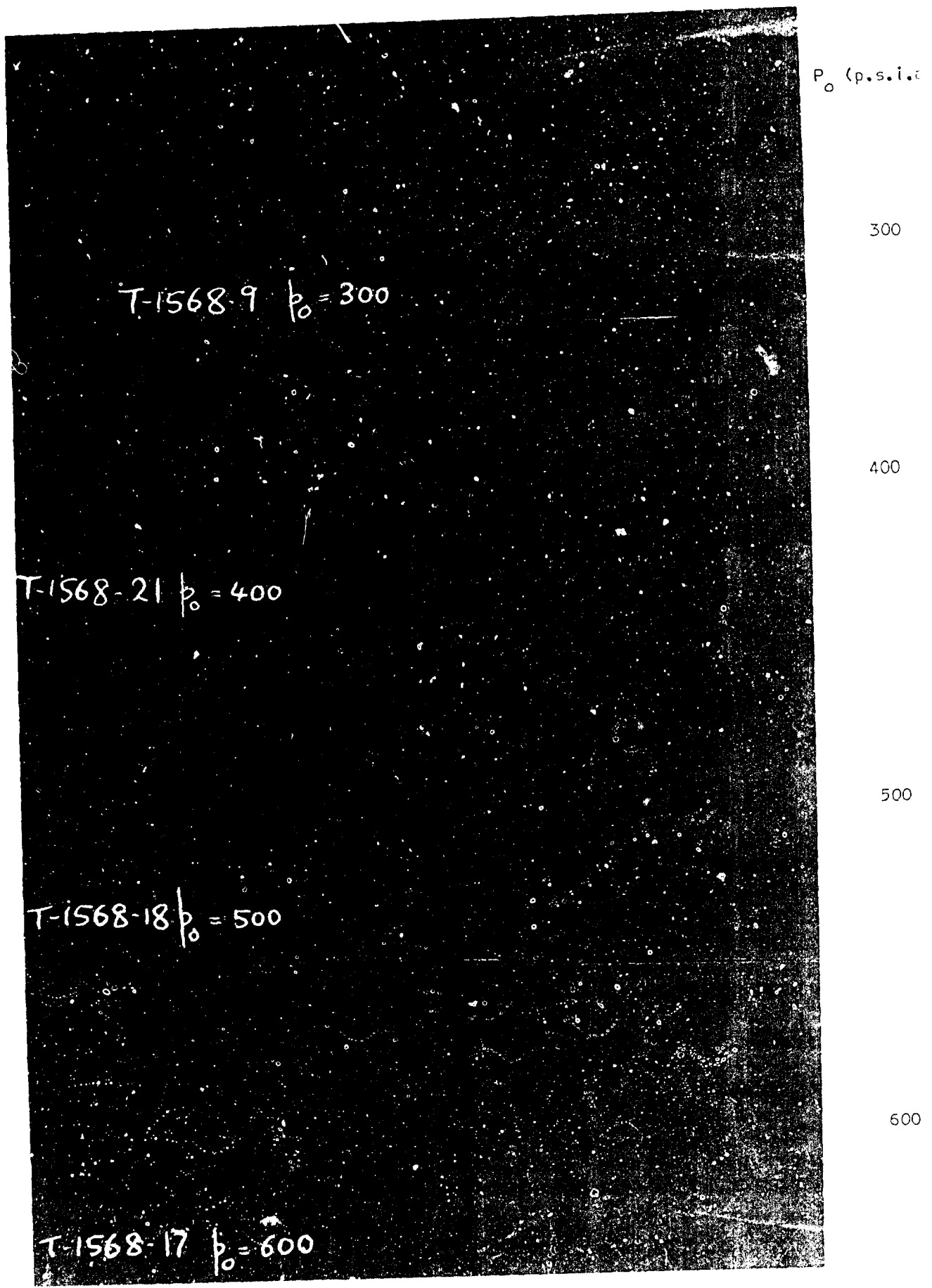
XII B3-14
 Figure 14.



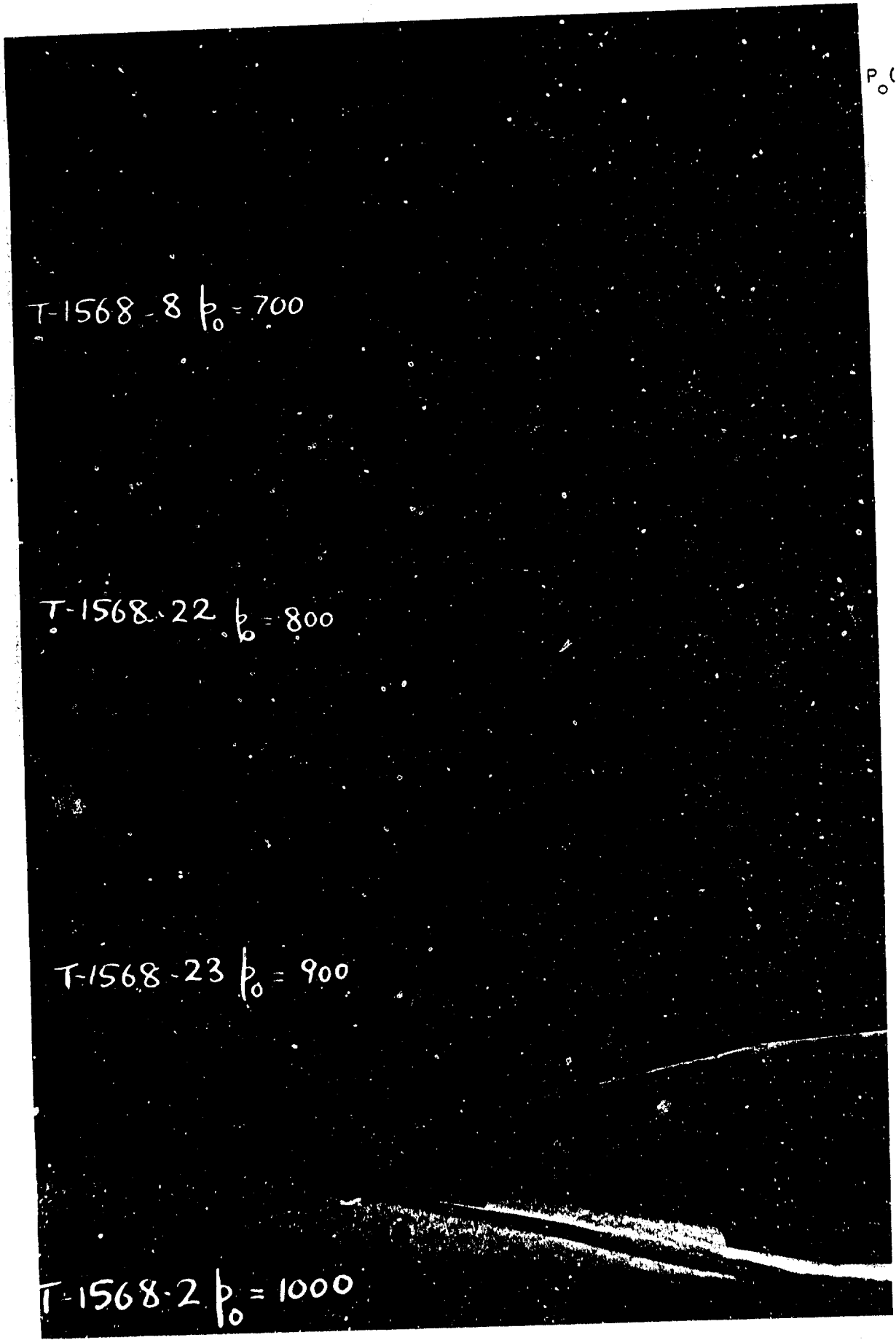
XII B3-15
 Figure 15.



XII B3-16
 Figure 16.



Schlieren photographs of 1 1/4" x 3/32" cavity model
at various stagnation pressures; $T_0 = 535^\circ R$.



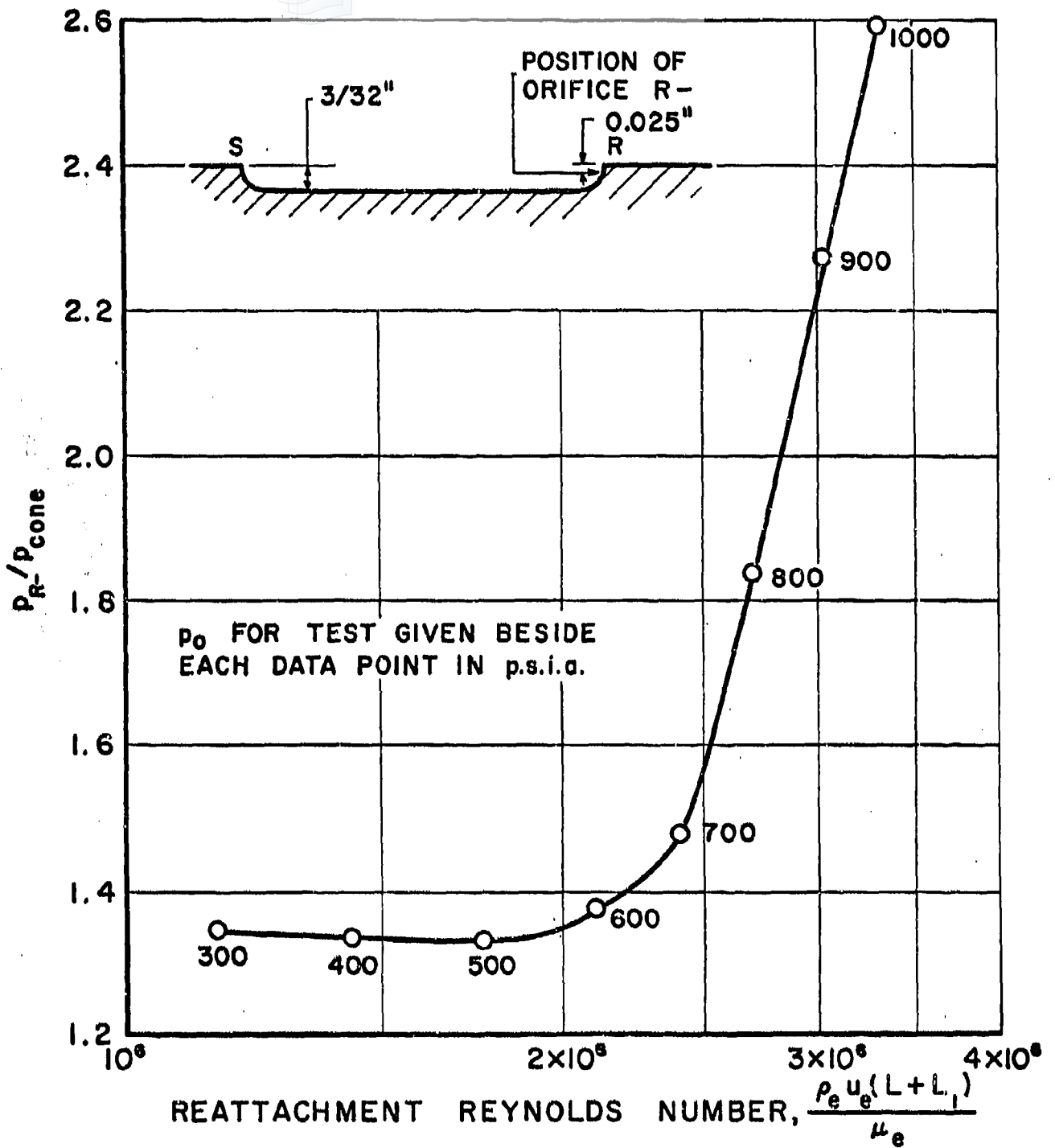
P_0 (p.s.f.a.)

700

800

900

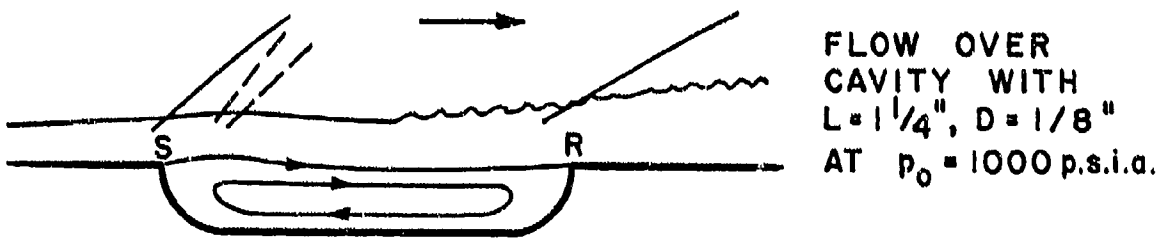
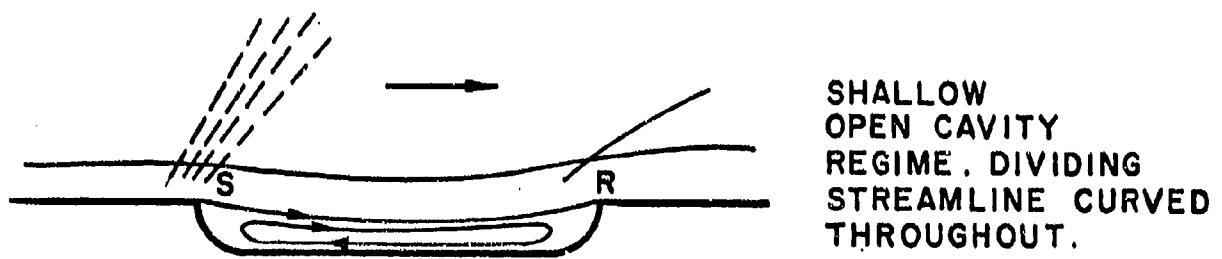
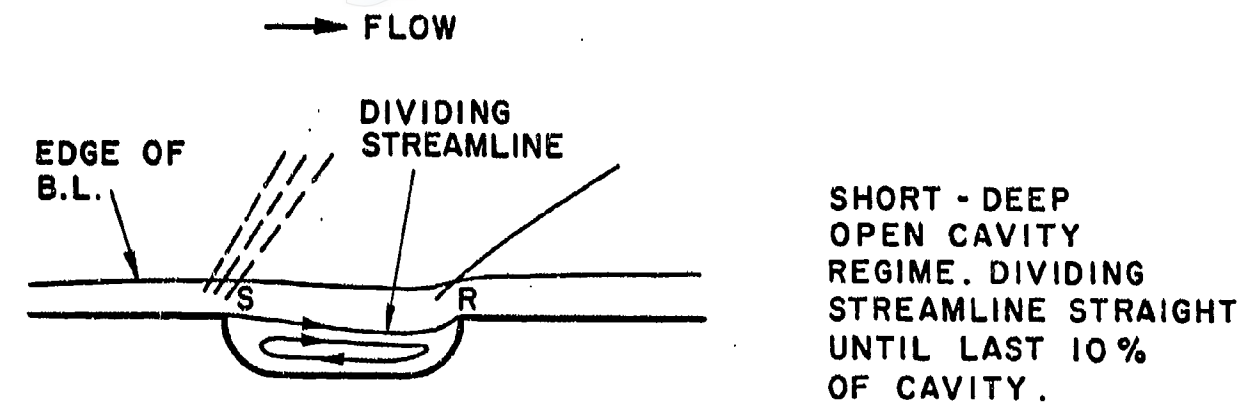
1000



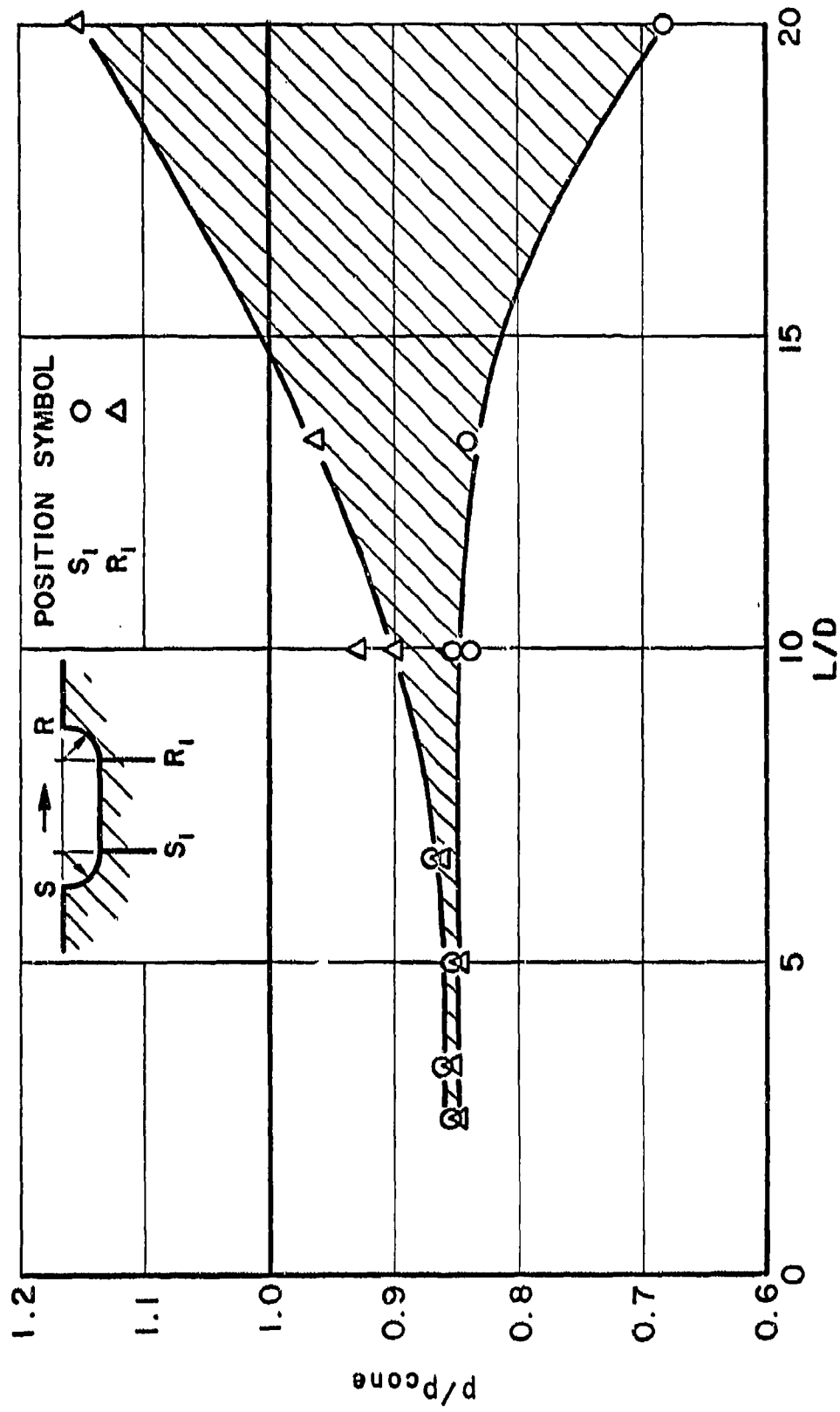
VARIATION OF REATTACHMENT PRESSURE WITH REYNOLDS NUMBER. $L=1\frac{1}{4}$ ", $D=3/32$ "

XII B3-17

Figure 18.



DIAGRAMS OF PROBABLE STREAMLINE PATTERNS
FOR VARIOUS CAVITY-FLOW TYPES
VERTICAL SCALE EXAGGERATED



RANGE OF CAVITY FLOOR PRESSURE AGAINST CAVITY L/D RATIO.
 LAMINAR REGIME, $p_0 \sim 400$ p.s.i.a.

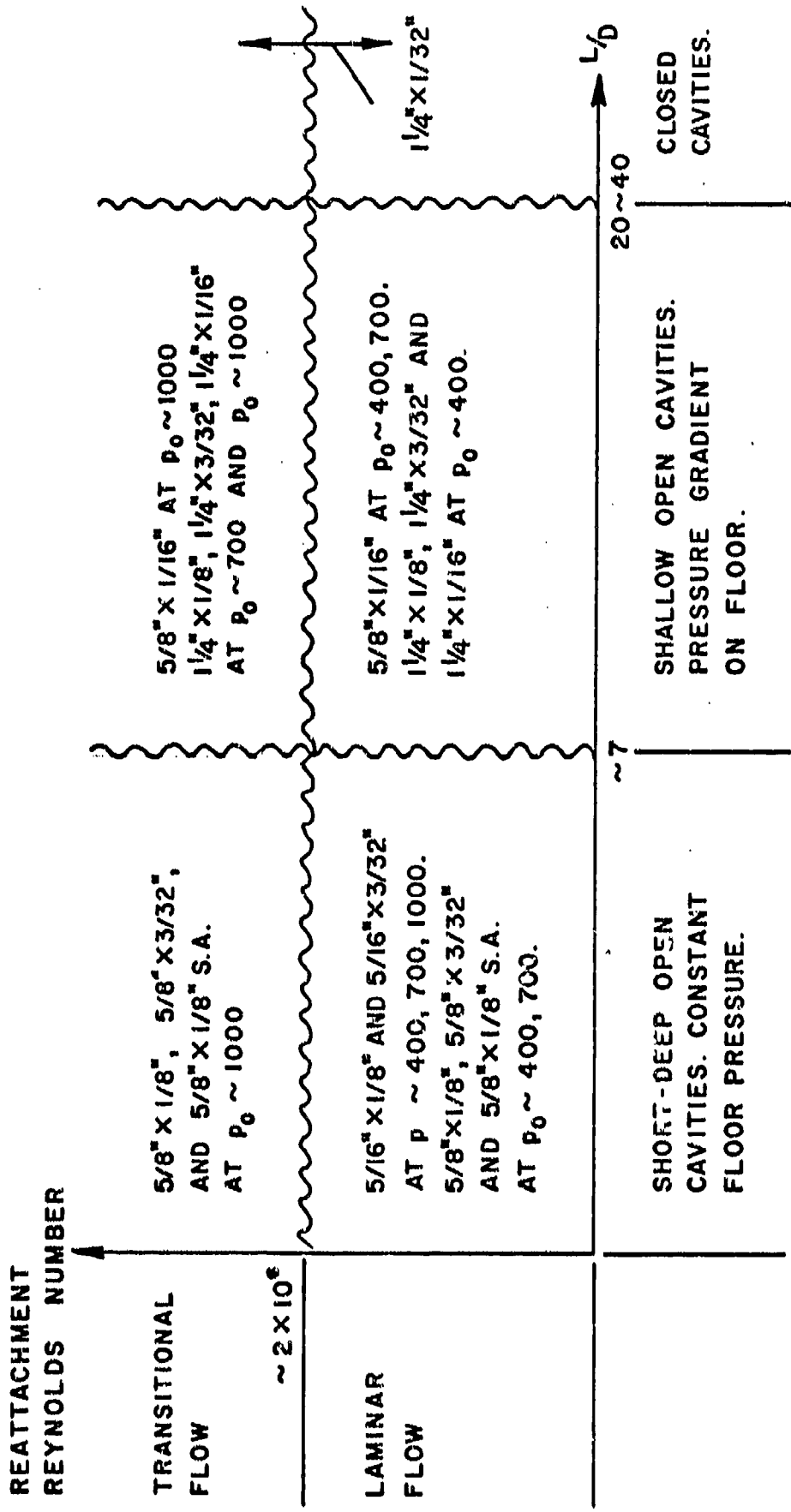
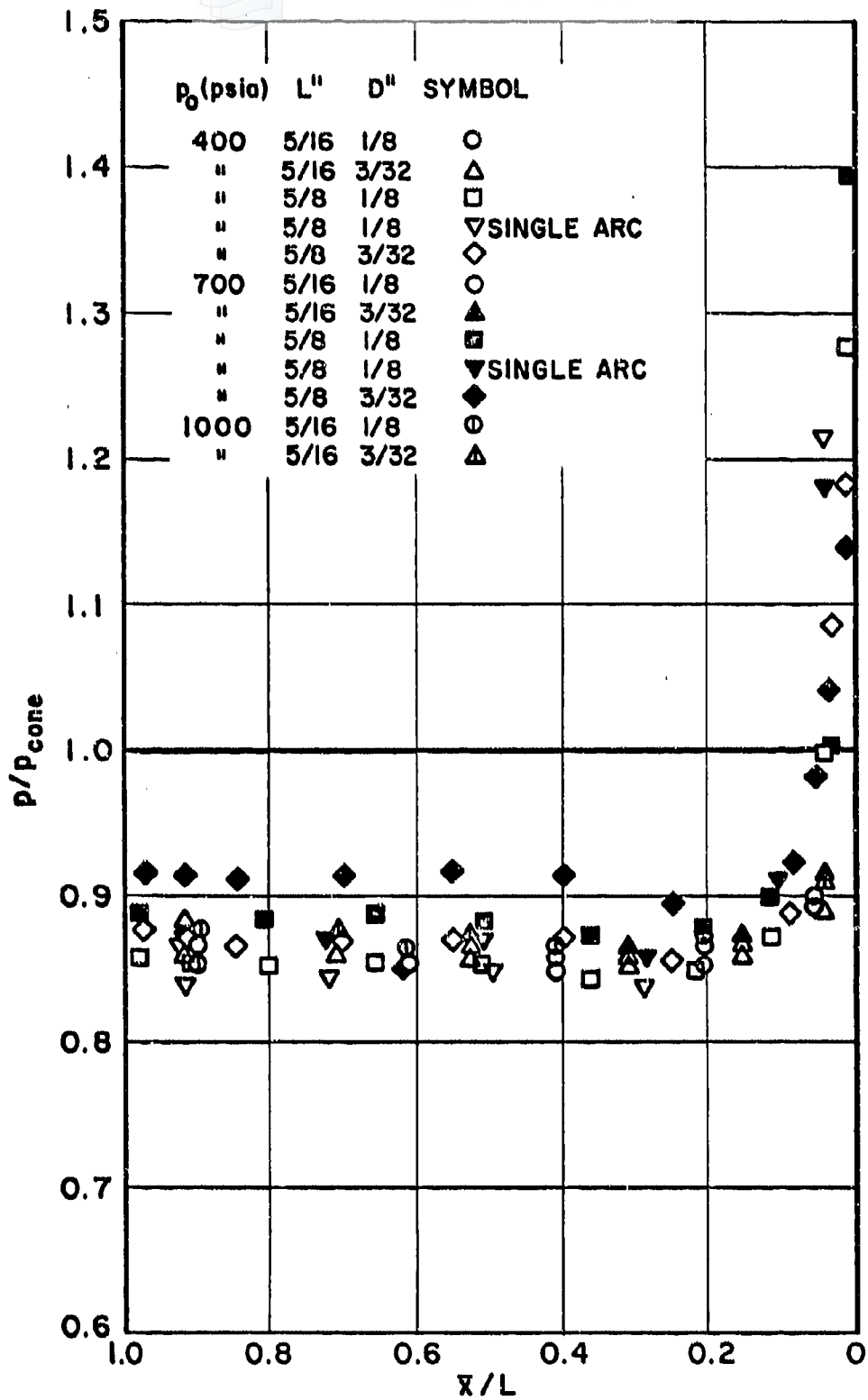


DIAGRAM OF CAVITY - FLOW REGIMES



DISTRIBUTION OF PRESSURE WITHIN CAVITY IN
 "SHORT-DEEP" REGIME CAVITY FLOW OPEN AND LAMINAR

XII B3-21

Figure 22.